Transcranial electrical stimulation devices

Dennis Q. Truong, Niranjan Khadka, Angel V. Peterchev, and Marom Bikson

The Oxford Handbook of Transcranial Stimulation, Second Edition (2nd edn)
Edited by Eric M. Wassermann, Angel V. Peterchev, Ulf Ziemann, Sarah H. Lisanby, Hartwig R. Siebner, and Vincent Walsh

Subject: Neuroscience, Cognition and Behavioural Neuroscience, Neuroscientific Techniques
Online Publication Date: Oct 2021 DOI: 10.1093/oxfordhb/9780198832256.013.2

Abstract and Keywords

Transcranial electrical stimulation (tES) devices apply electrical waveforms through electrodes placed on the scalp to modulate brain function. This chapter describes the principles, types, and components of tES devices as well as practical considerations for their use. All tES devices include a waveform generator, electrodes, and an adhesive or headgear to position the electrodes. tES dose is defined by the size and position of electrodes, and the waveform, duration, and intensity of the current. Many sub-classes of tES are named based on dose. This chapter focuses on low intensity tES, which includes transcranial direct current stimulation (tDCS), transcranial alternating current stimulation (tACS), and transcranial pulsed current stimulation (tPCS). tES electrode types are reviewed, including electrolyte-soaked sponge, adhesive hydrogel, high-definition, handheld solid metal, free paste on electrode, and dry. Computational models support device design and individual targeting. The tolerability of tES is protocol specific, and medical grade devices minimize risk.

Keywords: tES, neuromodulation, hardware, electrode, FEM, electrochemistry, skin, current flow, sensation, design

Disclosure: The City University of New York (CUNY) has IP on neuro-stimulation systems and methods with authors NK and MB as inventors. MB has equity in Soterix Medical. AVP received royalties, consulting fees, and/or grants from Rogue Research, Tal Medical/Neurex, Magstim, MagVenture, and Neuronetics. MB served on the advisory boards, received grants, and/or consulted for Boston Scientific, Mecta, Halo Neuroscience, and GlaxoSmithKline Inc. DQT has no conflict to declare.

Basics of tES devices and dose

A transcranial electrical stimulation (tES) device is essentially a current source connected to electrodes on the subject's scalp. tES dose is defined as the current waveform applied to the body and the number, shape, and location of electrodes placed on the scalp

that guide the waveform into the head. A practical tES device is equipped to reliably deliver the dose, including any operator controls, safety features, and instructions for use. The electrode number, shape, and location are collectively the montage. There is a minimum of two electrodes. One, if not all, electrodes are on the head. The waveform is produced by a powered device that can be directly attached to the electrodes, integrated into a headgear that includes the device and electrodes, or at some distance from the electrodes and connected to the electrode by lead wires (a benchtop or hand-held device; Fig. 1). Other than the waveform, device features such as shape, weight, power supply, user interface, and so on, are not explicitly part of the dose, but can be critical for usability (e.g., ability to apply correctly, acceptability, and compliance). Electrode design (e.g., materials) is reported separately from montage and waveform, but a central theme here is that because of reproducibility, usability, and tolerability factors, electrode design critically informs possibly both dose and device form (usability) factors.

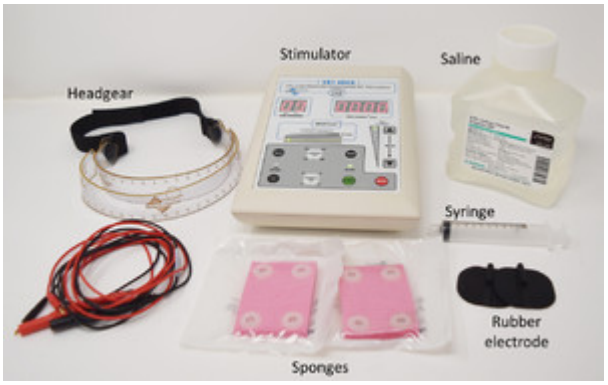

Figure 1 Example of a tES device (tDCS) and materials used for electrical stimulation with sponge electrodes. Generally, conventional sponges are soaked with a controlled volume of saline using a syringe. Rubber electrodes are placed inside the sponge pockets. Sponge electrodes are then secured on the scalp using a headgear. The rubber electrodes are energized using corresponding anode and cathode wires connected to the stimulator.

Sub-classes (non-commercial terms used in publications) of tES are typically defined by dose and/or intended use (Bikson *et al.* 2019). Device form factor and electrode design that are unrelated to dose are rarely explicitly part of tES classification; however, tES classifications are often associated with specific electrode design and device features. tES devices that deliver sufficiently high (hundreds of milliamperes) intensity in order to stimulate neurons in the brain above the threshold for action potential generation are typically denoted with the all-capital acronym “TES.” These include Electroconvulsive Therapy (ECT) devices which deliver pulse trains that intentionally produce a seizure in patients under anesthesia (Peterchev *et al.* 2010; George, Taylor, and Short 2013; Bai *et al.* 2017). This chapter is largely focused on limited intensity devices that deliver dosage significantly below that needed to activate neurons or produce seizures. These tES devices typically generate waveforms with a peak intensity of a few milliamperes (Antal *et*

al. 2017; Bikson *et al.* 2018), so that stimulation is comfortable when applied to alert, awake individuals. In most cases stimulation is applied for several minutes (e.g., 20 minutes) using two electrodes (e.g., few cm^2 surface area) on the scalp. Therefore, often the distinguishing features of different sub-classes of tES are the waveform shape and electrode montage rather than the peak intensity or period of use.

When the waveform is sinusoidal alternating current (ac) stimulation, tES is classified as transcranial alternating current stimulation (tACS)—where the frequency can be varied. When the waveform is a train of pulses, tES is classified as transcranial pulsed current stimulation (tPCS). There are many variations (sub-classes) of tPCS waveform including differences in the pulse duration, polarity (monophasic or biphasic), and repetition frequency. When the waveform is a sustained direct current (dc), tES is classified as transcranial direct current stimulation (tDCS). Additional terminology refers to further variations in waveform such as transcranial random noise stimulation (tRNS), slow oscillating direct current stimulation (soDCS), or cranial electrotherapy stimulation (CES). It is important to recognize that the function and effects of a device is defined by the full details of dose, not by its classification (the name it is called). That is, two devices may have the same name but through varying waveforms produce different outcomes. Also, a single tES device may be programmable to deliver different waveforms, e.g., a tDCS mode and a tACS mode.

Many tES devices include an intensity ramp up and ramp down. The ramp up and down is considered to increase the tolerability of tES, as skin sensation can accommodate over time. For example, a tES device may implement a 30-second linear increase in amplitude at the start of a session.

tES devices that deliver low-intensity stimulation, such as tDCS, tACS, and tPCS, are typically battery powered. ECT devices and TES devices that apply brief high-intensity stimulation for neurophysiological evaluation are wall powered. In all cases, the current is applied through wires (leads) to electrodes. In addition to the current waveform, the electrode number and shape determine dose and, in some cases, further refine the device classification. For example, the use of arrays of small electrodes is classified as high definition (e.g., high-definition tDCS, high-definition tACS).

As noted, all tES devices have a minimum of two electrodes, with at least one electrode placed on the scalp. At an anode electrode, current enters the body, and at a cathode electrode, current exits the body (Merrill, Bikson, and Jefferys 2005). At any instant of stimulation, there must be at least one anode and one cathode. For tES devices where the waveform polarity is fixed, such as tDCS and monophasic tPCS, each electrode has a fixed assignment of anode or cathode. For tES devices where the waveform is biphasic, such as tACS and biphasic tPCS, each electrode alternates between functioning as an anode or a cathode. When there are two electrodes, the current at one electrode is always the opposite of the other (1 mA at a single anode, indicates −1 mA at a single cathode). When there are more than two electrodes, the summed current across anode electrodes must equal the summed current across the cathode electrodes (Dmochowski *et al.* 2011)—that

is because the total current entering the body must equal the total current exiting the body.

Additional tES nomenclature

Based on the instant polarity of each electrode, an electrode can be described as an anode or cathode. In the case of tDCS the polarity of each electrode is fixed such that there is an anode electrode and a cathode electrode. However in all applications or tDCS, since an anode and cathode are always present, the terms “anodal-tDCS” or “cathodal-tDCS” refer to a hypothesis that neurophysiological or behavioral changes reflect neuromodulation of brain regions near either the anode or cathode, respectively (Garnett *et al.* 2015; Woods *et al.* 2016). The terms “reference” or “return” electrode refer to a hypothesis that brain regions near these electrodes are not central in any neurophysiological or behavioral changes. However, during tES current passes through all brain regions between electrodes and there is no inert electrode (Datta *et al.* 2009a; Opitz *et al.* 2015; Huang *et al.* 2017a). An extracephalic electrode indicates a position on or below the neck, which does not cancel the effect of this electrode, and rather produces current flow through the ventral surface of the brain and deep brain structures (Bikson *et al.* 2010; Noetscher *et al.* 2014).

Pulses are a common waveform used in tES, including by definition in all tPCS. Pulses are applied repetitively in a train, where the inverse of the time between pulses equals the stimulation frequency. Individual pulses are typically rectangular. Individual pulses have a pulse duration and amplitude. A waveform of pulses can be monophasic or biphasic. Monophasic waveform has pulses of a single polarity (Fig. 2A; $z_2 = 0$), while a biphasic waveform has pulses that invert polarity, typically in paired opposite polarity pulses (Merrill, Bikson, and Jefferys 2005). Wave types besides pulsed typically take the form of a simple periodic waveform, such as sinusoid (Fig. 2D). In the case that pulses are not evenly spaced in time, any burst patterns (Fig. 2B) or on/off times (Fig. 2c) are reported.

When waveforms are monophasic, asymmetric biphasic, or symmetric biphasic, but with importance of phase (pulse order), then the polarity of the waveform needs to be defined with respect to the electrodes (e.g., monophasic square wave with 5 V peak from electrode A to electrode B). In some cases, like bilateral monophasic stimulation, “anodal” and “cathodal” indicate the polarity of the waveform relative to the head (e.g., an electrode was placed on each mastoid with anodal right stimulation). In some applications where biphasic stimulation is used (such that each electrode can alternate between anode and cathode), the terms “anodic phase” and “cathodic phase” will be used (e.g., a cathodic phase pulse is followed by an anodic phase pulse). In this sense, when brain stimulation (Merrill, Bikson, and Jefferys 2005) is assumed to be driven by one phase, the terms “anodic stimulation” and “cathodic stimulation” are used (e.g., monopolar biphasic cathodic stimulation, where a cathode activating pulse is followed by an anodic phase used for charge recovery). However, here again these terms are statements of hypothesis in regard to the relative importance of each stimulation phase.

The terms “bipolar” and “unipolar” denote electrode geometry (independent of waveform). Unipolar electrode geometry typically refers to the use of a relatively small electrode placed near the target, with another (larger) “return” electrode placed at a distance. The idea being that the small electrodes govern neuromodulations and so the waveform (e.g., phase) is defined relative to the smaller electrode and the nominal target is near the smaller electrode. However, while the concept is well-established for invasive stimulation, for tES the role of relative electrode size may be muted. A bipolar electrode geometry indicates that two electrodes of comparable size are placed either around one nominal target or near two targets. When electrodes are placed symmetrically on the head, especially to target structures in both hemispheres, the montage may also be referred as bilateral. When two electrodes are used for a bilateral montage, it also bipolar. To clarify, biphasic/monophasic refer to waveform and are independent of bipolar/unipolar/bilateral electrode geometry.

More classifications and tES-specific terminology can be found in literature, not all of it used consistently or clearly (e.g., “dual-tDCS” vs “Dual-site high-definition tDCS”). For some subclasses, terminology takes on specific connotations (e.g., bilateral ECT). The same dose may be referred to by varied classifications. In light of ambiguity in terminology, one should always refer to the dose of the device. To the extent the dose if not specified fully, a publication (or device performance) cannot be reproduced. tES nomenclature is discussed in more detail in Bikson et al. (Bikson *et al.* 2019).

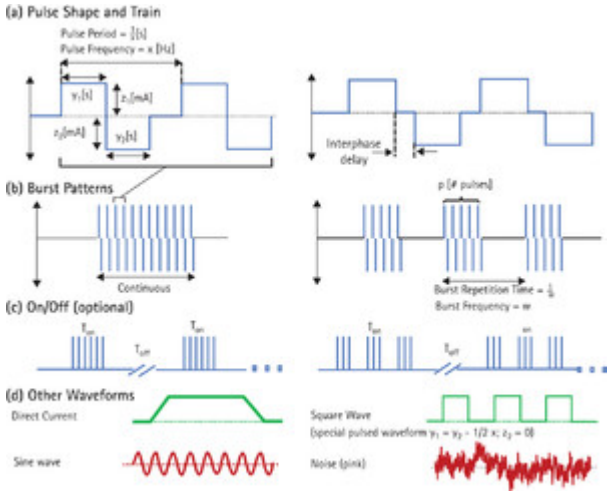

Figure 2 Different types of waveforms used in tES and their parameters. (A) Rectangular biphasic pulses with frequency “x (Hz),” period “1/x (s),” amplitude “$Z_1 = Z_2$ (mA),” and pulse width “$y_1 = y_2$ (s).” (B) Burst patterns of pulses (continuous or discrete) where “P” is number of pulses, “w” is the burst frequency, and “1/w” is burst repetition time. (C) Monophasic burst on (T_{on}) and burst off (T_{off}). (D) Other waveforms such as direct current (DC), square wave, sinusoidal, and pink noise.

tES electrodes: General considerations

The key technical contributors to the broad adoption of tES are the portability and ease of use, along with the tolerability profile of most tES techniques. For limited intensity tES techniques, adverse events are largely limited to effects that occur at the skin such as transient cutaneous sensations (e.g., perception of warmth, itching, and tingling) and erythema (Dundas, Thickbroom, and Mastaglia 2007; Fertonani, Ferrari, and Miniussi 2015; Aparício *et al.* 2016; Bikson *et al.* 2016). Because these minor adverse events are limited to the skin, the design and preparation of tES electrodes is considered central to tolerability. Electrode design, in turn, can govern which waveforms will be tolerated. Indeed, it is only when established electrode protocols are not followed or poor electrode design used, that tES produces unnecessary significant skin irritation and burns (Dundas, Thickbroom, and Mastaglia 2007). In addition, electrodes underpin reliable dose delivery and electrode design increasingly emphasizes ease and robustness of use (e.g., potential for home use). For clinical trials, since sensations determine effective blinding, tES electrodes also impact blinding reliability. Finally, to the extent tES electrodes design—separate from montage which evidently matters—shapes current flow through the brain (Opitz *et al.* 2015), electrode selection and preparation is critical for reproducibility and efficacy.

Regarding montage, the typical tES devices utilizes two electrodes of comparable size, each positioned on the head (DaSilva *et al.* 2011; Nasseri, Nitsche, and Ekhtiari 2015; Woods *et al.* 2016). However, strategies with asymmetric electrode size, an electrode at or below the neck (Bikson *et al.* 2010), or increasing number of electrodes (e.g., using high-definition electrodes) have been investigated to alter tES spatial focality (Monte-Silva *et al.* 2010; Minhas *et al.* 2012; Galletta *et al.* 2015).

In the electrochemistry literature, an electrode technically refers only to the surface of metal or conductive rubber that makes a contact with an electrolyte, such saline or conductive gel (Merrill, Bikson, and Jefferys 2005). However, in the tES literature, an electrode conventionally refers to the totality of the entire electrode assembly that includes: 1) the electrochemical electrode (metal disk, sheet, mesh, or conductive rubber); 2) a conductive electrolyte such as the saline, conductive paste, or conductive gel that serves as the contact between the electrode and the skin; 3) any nonconductive material that is used to support or hold the electrolyte such as a sponge of plastic high-definition support; 4) any conductive components used to connect the electrode with the device or leads such as metal snap or pin; and 5) additional nonconductive support material such as insulative backing or adhesive. Throughout this review, electrode thus indicates electrode assembly, while electrochemical electrode indicates the metal or conductive rubber. The electrolyte shape and formulation are critical for tolerability, since the electrolyte is typically the only conductor that should make contact with the skin in most tES techniques (ECT is an exception where in some cases metal electrodes may contact the skin directly). While the shape and size of tES electrodes is often reported as that of the electrode hardware itself, it is the electrolyte–skin interface that determines where current enters the body and therefore the dose. Thus, the electrolyte–skin interface is critical to control and document, especially in cases where the electrolyte spreads beyond the hardware elec-

trode area. The nonconductive or conductive-connective components of the electrode assembly serve a mechanical or usability purpose. The electrochemical electrode affects tolerability by how it interacts with the electrolyte during stimulation.

Single use electrodes are advantageous. In any case, the electrolyte should not be reused; as an electrolyte dehydrates its properties will change, impacting quality of contact with the skin, and therefore tolerability. Electrodes, with special emphasis on the electrolyte–skin interface, are positioned on the head using various techniques. Electrodes can be positioned based on head anatomical landmarks. These can be modestly sophisticated requiring a trained operator, for example using the EEG 10–10 system (e.g., anode on C3). While more simplistic placement techniques are based on gross anatomical landmarks (e.g., over the eyebrow). When a head gear is used, it is either designed to support the determination of specific electrode positions (e.g., a cap or marked straps (Schestatsky, Morales-Quezada, and Fregni 2013; Kasschau *et al.* 2015)), or the headgear is used for generic mechanical support (e.g., rubber bands (DaSilva *et al.* 2011)) and so an independent measurement is used to position the electrodes. More sophisticated placement techniques include neuronavigated (Richardson *et al.* 2015; Teichmann *et al.* 2016; Parazzini *et al.* 2017; De Witte *et al.* 2018), functional (Rich *et al.* 2017), nonneuronavigated approaches that rely on general scalp landmarks (Seibt *et al.* 2015), or image-based approaches (e.g., EEG reciprocity (Fernández-Corazza *et al.* 2016; Wagner *et al.* 2016; Dmochowski *et al.* 2017; Leite *et al.* 2017)).

Across different tES approaches and positioning techniques, what matters first is the reproducibility of the dose. A relatively simplistic placement approach may be sufficient (e.g., centered on the forehead), as long as it can be reproduced. Though electrode contact quality (design, preparation, and application) is not explicitly part of dose, it underpins tolerability and also reproducibility. Regardless of if a study meets its primary endpoint or not, without reproducible dose, it has minimal value. What matters next is how the positioning method reliably engages the neuronal targets responsible for the desired outcomes. In this sense, a very complex position system, which nonetheless results in inconsistent outcomes is not valuable. In this last sense, the method of electrode positioning is further intractably tied to the hypothesized mechanism of action. A further consideration for a positioning system is acceptability and compliance. Ultimately, an approach that is overly costly and cumbersome will not produce an effective intervention, especially in deployed environments such as home use. All these factors inform the design of devices, headgear, and electrodes, including labeled instructions for use.

tES electrodes are made from a conductive rubber or metal separated from the skin by a saline-soaked sponge, gel, or paste (Woods *et al.* 2016). As noted, in electrochemistry, the conductive rubber or plate would be the electrode, while the saline, gel or paste would be the electrolyte (Merrill, Bikson, and Jefferys 2005), whereas in the tES literature, the entire assembly is called the electrode. The electrochemical electrode is the interface between metal or rubber and the electrolytes and is where electrochemical reactions (e.g., pH changes) occur. As noted, in tES when electrode size is described (e.g., 5×5 cm^2), it is the interface area between the skin and the electrolyte. Nonetheless, the configuration

of all electrolyte and electrochemical electrode dimensions and materials are important to control and document as this affects tolerability (Dundas, Thickbroom, and Mastaglia 2007; Minhas, Datta, and Bikson 2011; Kronberg and Bikson 2012; Turi *et al.* 2014; Woods *et al.* 2016). The thickness of the sponge or paste effectively controls the minimum distance between the conductive rubber or metal and the skin. Contact of conductive rubber or metal with skin during tES is avoided as this compromises tolerability and introduces risk of significant skin irritation. This is the main reason why, the more involved an electrode preparation technique is, the more prone it is to setup error (e.g., insufficient electrolyte thickness in a free-paste electrode), the less deployable it is. When the electrodes are intended for wide or deployed use, they should require minimum preparation (e.g., adhesive electrodes, pre-saturated sponge electrodes).

There are two essential functions of the electrolyte, and by extension materials used to support the electrolyte shape such as sponge, hydrogel polymer, and/or other support materials that contain a viscous electrolyte (such as in the high-definition electrodes). Both functions of the electrolyte relate to preventing direct contact between the metal or conductive rubber electrode and the skin. The first function relates to electrochemical products, including changes in pH, that occur only at the interface between the metal or rubber and the electrolyte (Merrill, Bikson, and Jefferys 2005). Thus, a “thick” electrolyte (e.g., realized by a thick sponge, gel, or holder) minimizes these reactions from reaching the skin. The second function relates to normalizing current flow patterns through the skin. Related to this, the saline, conductive paste, or conductive gel is used to maintain good contact quality at the skin (Minhas *et al*. 2010; Woods *et al*. 2016; Khadka, Woods, and Bikson 2019). If, as result of poor electrode design (e.g., conductive metal or rubber not fully protected from the skin), or preparation (e.g., a metal or rubber electrode pushed through paste) the metal or rubber contacts the skin, the resultant electrochemical changes or poor current density patterns can adversely impact the skin and aggravated skin irritation is likely.

Thus, the cardinal function of electrodes used in tES is to protect the skin from electrochemical reactions occurring at the surface of the metal or rubber, to normalize current density across the skin (e.g., minimize hotspots), and to ensure reliable and tolerable current delivery into the body. Because electrochemical concerns are paramount, all electrodes designed for tES include some mechanism to separate the metal or rubber from the skin. The electrolyte, being the conductive element contacting the skin, thus takes an importance in general performance. As expanded in the following sections, the design of the electrolyte (including how distance between the metal or rubber and the skin is maintained) is thus central in the classification of electrode types:

1) Sponge electrode: a sponge saturated with the fluid electrolyte, typically saline, with a metal or rubber conductor inside the sponge (sponge pocket design) or on the sponge surface opposite the skin. The sponge sets the electrolyte shape and conductive path.

2) Self-adhesive integrated electrode: a hydrogel electrolyte that has sufficient rigidity not to flow or spread, and with the gel or material around the gel including an adhesive component.
3) High-definition electrode: a stiff mechanical support (short tube or cup) that contains the electrolyte, typically gel, and also controls position of the metal. Used for smaller electrodes and suitable for arrays.
4) Free electrolyte on hand-held conductor: “Free” indicates application by the operator without strict control of thickness by the electrode assembly. Re-used solid metal electrode, covered per-use with a thin electrolyte layer, and an operator handle to manually press down. Used in some forms of ECT and not considered further here.
5) Free paste on conductive rubber electrode: the paste may also provide adhesion. Used in some investigational forms of tDCS or tACS and not considered in detail here.
6) Dry electrodes: novel designs that are not adhesive and leave no residue (no liquid or paste).

These general design approaches have various performance tradeoffs on 1) the size of the electrode (e.g., small high-definition vs large sponge) which can impact the ability to leverage electrode arrays for targeting; 2) how much preparation is required and the need for headgear); and 3) if the electrodes can be applied on hair (see Table 1).

Table 1 Categories of tES electrodes and usability features.

Electrode Type	On hair?	Preparation?	Headgear required?	Focal optimization?	Electrode sizes
Sponge	Yes	Yes / No[Ƀ]	Yes	No	Large
Self-adhesive	No	No	No	No	Variable
HD	Yes	Yes[¥]	Yes	Yes	Small
Hand-held	Yes	Yes[¥]	No	No	Large
Free paste	Yes	Yes[¥]	No	No	Large
Dry	Unknown	No	Yes	No	Variable

(*) except if supplemented with additional preparation adding liquid gel

(Ƀ) for single-use pre-saturated snap design

(¥) including gel or paste residue clean-up

tES electrodes: Sponge electrode

This electrode type is the most common electrode design used in some tES techniques such tDCS, tACS, tRNS, and related techniques (DaSilva *et al.* 2011), where electrode positions over the hairline is common (Fig. 3). Adoption is largely due to its apparent simplicity, ability to be positioned over hair, and its use in tDCS and historically derivate approaches like tACS and tRNS (Nitsche and Paulus 2000). However, there are significant details in both the optimization of the sponge electrode design and techniques in sponge electrode preparation (Woods *et al.* 2016). Sponge electrodes require a headgear to hold them in place (as opposed to self-adhesive electrodes) and the design of the headgear itself requires nuanced consideration.

Most commonly in current tDCS, tACS, or tRNS protocols, a conventional sponge electrode pad has a square skin contact area of either 25 cm^2 (5 × 5 cm) or 35 cm^2 (5 × 7 cm) with the scalp, where this contact area is the interface between the electrolyte-saturated sponge and the skin. For sponge electrodes, selection and positioning of the conductive carbon rubber sheath or metal can be varied. For example, Soterix Medical (EasyPad, Soterix Medical Inc., NY, USA) provides a rubber electrode embedded inside a rectangular sponge pocket and uses plastic rivets to hold the rubber in place. In the Neuroconn sponge electrode (neuroCare, Munich, Germany), the rubber sheath is inserted into a sown rectangular sponge pocket. In both cases, the rubber electrode is smaller than the outer dimensions of the sponge. In the Amrex-style sponge electrode (Caputron, NY, USA) a metal electrode is placed behind the rectangular sponge, and an insulating rubber encases the metal and sponge, except on the skin contact side. These reusable conductive rubber electrodes typically include a female port which is connected to a male banana plug terminating the wire from the stimulator. CES devices can use circular sponges soaked in tap water (Fisher Wallace electrode, New York, USA). Relatively small disposable felt electrodes that are saturated in saline are used in some CES devices with ear clip electrodes (Alpha Stim, Texas, USA). Nonsalinized water is less common (and contraindicated (Woods *et al.* 2016)) in tDCS, with the salinized-sponge exception noted in the following section. In any case, when water is used residual electrolyte must be present either as impurities (tap) or absorbed from the skin.

There are updated variants of the sponge electrode design. The conductive rubber may be semi-permanently embedded into a circular (Sponstim, Neuroelectrics, Spain) or rectangular (EasyPad-2, Soterix Medical Inc., NY, USA) sponge with a male metallic connector attached to the rubber and emerging through the sponge (on the side opposite the skin contact). The male connector can be affixed to a female connector on the headgear directly. As with other sponge electrodes, the electrodes can be re-used or are single use. Single-use electrodes are further available as pre-saturated, thus requiring no preparation (Soterix EasyPad-2, Fig. 4). A further variation is a more rigid sponge with bristles that enhances preparation through hairs, and sponge materials embedded with salt in a manner that only water needs to be added over multiple uses (Halo Neuroscience, San

Francisco, CA). Along with new types of associated headgear (e.g., for home use (Kasschau *et al.* 2015)) and connectors (e.g., magnetic), these examples illustrate that even with the conventional sponge electrode paradigm, there is an ongoing innovation often focused on ease of use (e.g., pre-assembled and saturated) or reliability (e.g., sponge surface shape).

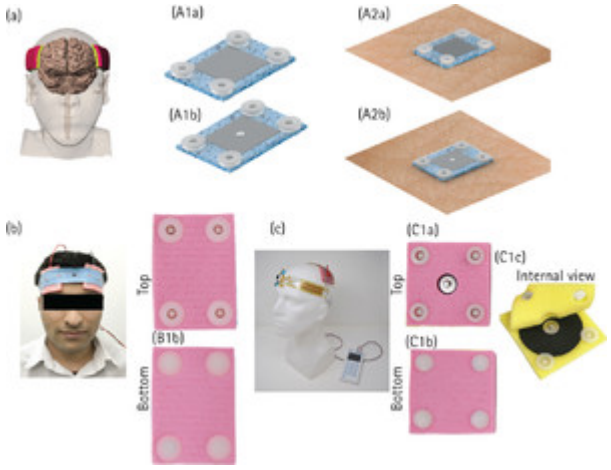

Figure 3 Architecture of sponge electrode and its variations. (A) An exemplary FEM model of sponge pad positioning over left and right dorsolateral prefrontal cortex (dlPFC) in a head model. (A1a, A1b) CAD exemplars of sponge assembly variations where in both the rubber electrode is placed in between two layers of sponges, except the later has metal snap on top of the rubber (see C1c) to facilitate connection with customized headgear (head strap). Both variations of sponges have rivets to minimize edge effects, hence maximizing tolerability. (A2a, A2b) show models of the sponge pads positioned over the skin surface. (B) Bifrontal placement of riveted sponge electrode (as in A1a) on a subject's forehead. (B1a, B1b) Images of actual sponge electrode (5 × 5 cm) as used in B1. (C) illustrates positioning of updated snap-in sponge electrode assembly on a fixed montage-specific head gear, in this case M1–SO. (C1a, C1b) depict different views of the snap-in sponge electrodes (5 × 5 cm) as in A1b. The shape of the rubber electrode does not influence the total current delivery to the brain region. (C1c) illustrates internal view of the snap-in sponge electrode where the circular rubber electrode is placed exactly at the center of the sponge pad.

Sponge electrodes are intended to increase the contact quality even in the areas of the scalp with thick hairs because the electrolyte (saline) penetrates the hair and saturates the skin surface. Theoretically, the saturation of skin may also reduce inhomogeneity in the current flow through the skin (Kronberg and Bikson 2012). Some disadvantages of using sponges are that sponge is prone to leaking which distorts the "effective" electrode size making stimulation not reproducible (Woods *et al.* 2016). For this reason, the volume of saline added to the sponges should be carefully calibrated (to the sponge model, size,

and application) and caps (e.g., neoprene) may be avoided since it both obscures and supports fluid spread.

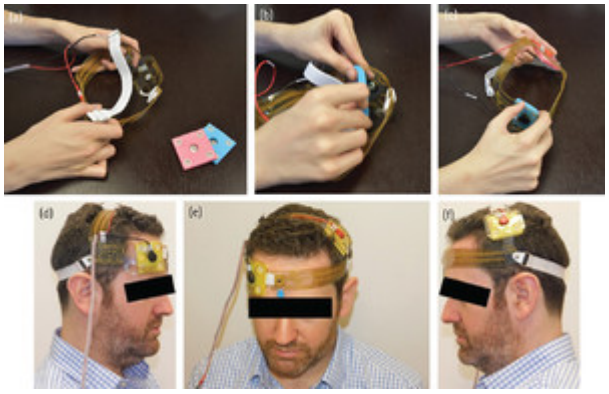

Figure 4 An updated method for electrode placement using fixed position headgear and pre-saturated snap sponge electrode. (A) Example of a headgear with built-in anode and cathode snap-in wire terminals at fixed positions (M1–SO montage). (B) Pre-saline-soaked sponges with snap connectors are affixed to the anode or cathode terminals. (C) Complete assembly of sponge electrodes and headgear. (D, E, and F) Different views of head-strap placement on a subject's head.

Sponge electrode of various sizes have been used for tDCS, tACS, and tRNS (including 3 × 3, 5 × 5, 5 × 7, 10 × 10 cm) but smaller sponge sizes are not practical or necessarily tolerated (but see high-definition electrodes). Neither changing the sponge–skin contact shape from square to circular (Ambrus, Antal, and Paulus 2011; Minhas, Datta, and Bikson 2011) nor changing sponge–skin contact size within the conventional range (Turi *et al*. 2013) had significant effect on tolerability (Fertonani, Ferrari, and Miniussi 2015; Aparício *et al*. 2016). Apparently, more important than electrode–skin contact area and shape is the electrode design, such as material thickness and use of rivets (Kronberg and Bikson 2012) as well as electrolyte salinity (Dundas, Thickbroom, and Mastaglia 2007). However, changes in electrode shape and size (Nitsche *et al*. 2007), and even design (Opitz *et al*. 2015), may influence brain current flow and therefore outcomes.

tES electrodes: Self-adhesive electrode

Self-adhesive electrodes adhere to the skin surface and require minimal preparation, making them easy to use at locations without significant hair (Paneri *et al*. 2016). They are typically, but not exclusively, used with tPCS waveforms. The bottom of the electrode has a layer of conductive hydrogel along with an adhesive material. Over the hydrogel is conductive rubber or metal that is connected to a conducting wire. Finally, there is an insulation material that wraps the electrode assembly, except where skin contact is made (see Fig. 5D2). In some designs, the metal may be connected to a short, insulated wire with a female pin connection (the cable from the stimulator can be connected to this fe-

male pin) or the metal may be connected to a snap connector that protrudes through the insulation layer. When the device is hand-held the lead wire from the device extends to the connector on the electrodes. When the device is wearable, it may connect directly to the adhesive electrode and the adhesion may be sufficient to hold the device on the head.

Because dc stimulation is electrochemically demanding (Minhas *et al.* 2010), adhesive electrodes have been used in a limited number of tDCS trials (Paneri *et al.* 2016) and devices (Zendo E-Meditation, New York, USA), but are common in other applications where biphasic pulses or ac stimulation are used, such as cranial nerve electrical stimulation (Feusner *et al.* 2012). Although self-adhesive electrodes are easy to apply, their use is limited for stimulating areas of the head with hairs. While there are many brands and designs of self-adhesive electrodes, those designed for recording (e.g., echocardiogram (EKG)) may not be suitable for electrical stimulation. Moreover, electrodes designed and validated for one stimulation dose may not be tolerated for other doses.

For ECT special self-adhesive electrodes may be used (Thymapad, Somatics, FL, USA), with the constraint noted previously on off-hair placement. As a result, bilateral or bifrontal ECT montages using adhesive electrodes may in fact result in electrodes placements distinct from standard configurations using hand-held electrodes that can go over the hairline.

Many approaches that use adhesive electrodes for head stimulation are intended to activate cranial (or peripheral nerves); as such these are not “transcranial” techniques and are, therefore, outside the scope of this chapter. Nonetheless, insights from cranial stimulation devices can inform tES devices. Cranial nerve stimulation devices have used handheld designs (Monarch, NeuroSigma, CA, USA) as well as compact devices that snap directly to the adhered electrodes (Thync pad, CA, USA and Cefaly, CT, USA), making the entire system wearable. Technologies intended to stimulate cranial nerves can have electrodes of varied separation, ranging from distant electrodes across the head, to proximal (adjacent) electrodes. The latter case produces local superficial current flow suited for stimulation of cranial nerves at the skin, but not transcranial. In the former case, the two distant electrodes are presumably stimulating two targets, through there is also increased transcranial current through the head. For this reason, transcranial systems with adhesive electrodes avoid adjacent electrode placement (e.g., placed at a distance across the forehead) (Paneri *et al.* 2016). These last points relate to a broader debate within the field of noninvasive neuromodulation (Asamoah, Khatoun, and Mc Laughlin 2019); regardless of whether a system is called “transcranial” or claimed to target cranial nerves, there can be a significant overlap in dosage between such systems. Without verification of target engagement—i.e., what nervous system elements are activated and correlated with outcomes—the targets of these devices can be speculative. For CES devices, which include models of adhesive electrodes (Caputron, Mindgear, NY, USA), the targets may be cranial nerves, the brain (Datta *et al.* 2013a), or a combination of both.

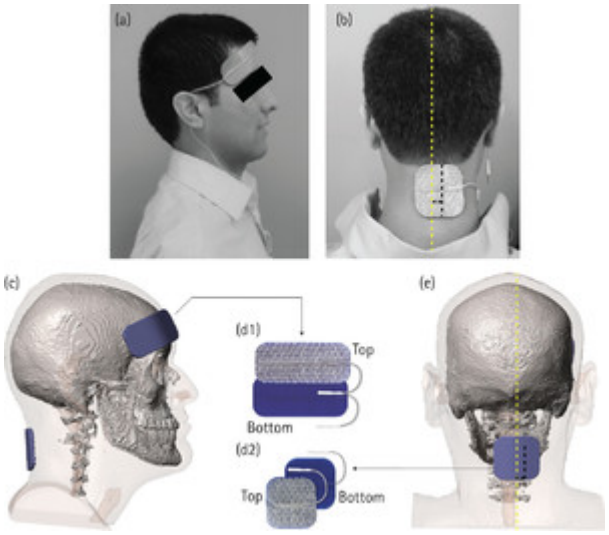

Figure 5 Illustration of adhesive hydrogel electrode. (A) Placement of a rectangular anode on the subject's right temple. (B) A square cathode electrode positioned about 1 cm to the right of the subject's midline on the back of the neck. (C, E) Representation of analogous electrode positioning as A and B on a realistic head model. (D1, D2) Actual images of the two adhesive electrodes. The bottom (skin side) of the electrode has an adhesive hydrogel to enhance adherence with the skin, whereas at the top, there is a mesh of conductive fabric covered by insulator.

tES electrodes: High-definition electrode

High-definition electrodes are electrode assembly with a skin contact area of less than 5 cm^2. The high-definition electrode includes a cup that sits on the skin and determines the skin contact area. The cup is filled with a conductive gel or paste (Minhas *et al.* 2010). Suspended inside the gel is a metal ring, disk or pellet made from Ag/AgCl. The gel and metal are thus confined by the interior dimensions of the high-definition cup. The design of the high-definition cup controls the important factors of gel contact area with the skin and the distance between the metal and the skin (Fig. 6A). As with conventional tDCS using sponge electrodes, there are different montages of high-definition tDCS. However, high-definition electrodes, by the virtue of being smaller, can be deployed in significantly higher number and/or precision of placement (Dmochowski *et al.* 2011; Borckardt *et al.* 2012; Kuo *et al.* 2013). A common high-definition montage is the 4×1-ring configuration where four "return" disk electrodes encircle an "active" electrode at the center (Datta *et al.* 2009a; Alam *et al.* 2016; Shen *et al.* 2016; Hill *et al.* 2017) (Fig. 6 B,C). The return electrodes are at a distance of approximately 3–5 cm from the active electrode (disk center to disk center). The high-definition electrodes are held in place using a cap head gear and a conductive electrolytic gel is filled into the electrode holders. Note that, in contrast to sponge electrodes (Woods *et al.* 2016), here a cap does not introduce issues related to

electrolyte spread since the gel is well confined by the high-definition cup (Villamar *et al.* 2013a).

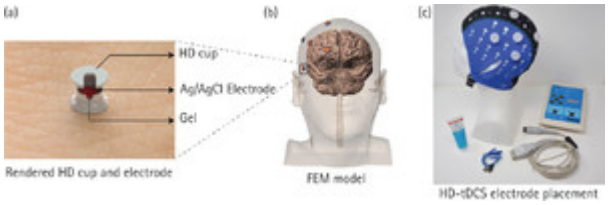

Figure 6 Positioning of high definition (HD) electrodes on head. (A) HD-cup with an electrode submerged in a conductive gel. (B) Model of a 4 × 1-ring configuration where four "return" electrodes are positioned around a central "active" electrode. (C) Illustration of HD-electrode assembly on a subject's head. The electrodes are secured in a 4 × 1 configuration using a specialized head cap that follows standard EEG electrode positioning.

Various waveforms can be applied in high-definition tES. High-definition tDCS uses dc waveforms (Borckardt *et al.* 2012; Caparelli-Daquer *et al.* 2012; Kuo *et al.* 2013; Villamar *et al.* 2013b) whereas high-definition tACS uses ac waveforms (Helfrich *et al.* 2014; Bland, Mattingley, and Sale 2018; Reinhart and Nguyen 2019). High-intensity pulses for suprathreshold stimulation of the cortex can be applied through high-definition electrodes as well (Edwards *et al.* 2013). High-definition electrodes are also well suited for other waveforms such as interferential stimulation (Grossman *et al.* 2017) that require multi-electrode arrays. Finally, multiple brain regions can be targeted simultaneously with high-definition tES (Hill *et al.* 2018; Meier *et al.* 2019; Reinhart and Nguyen 2019) (Fig. 7).

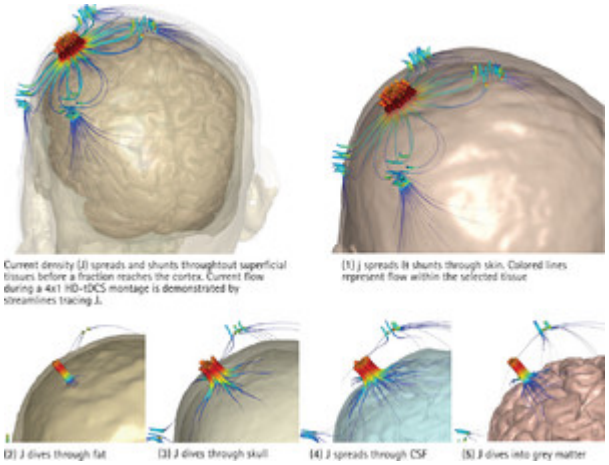

Figure 7 Illustration of current spreading and shunting through superficial tissues. Only a fraction of the current delivered during tES reaches the cortex. In the 4 × 1 HD-tES example, the center and surround electrodes are in close proximity on the scalp surface. Much of the current shunts though skin, but a fraction of the current spreads into deeper tissues and eventually into the cortex.

The form factor of high-definition tES cups superficially resembles EEG electrodes (though EEG electrodes cannot be reliably used for stimulation), and indeed it is possible to combine high-definition tES and EEG systems. However, while EEG recoding before high-definition tES (for example to measure baseline brain state of inform stimulation strategy (Dmochowski *et al.* 2017; Thut *et al.* 2017)) or after high-definition tES (to measure outcomes (Heimrath *et al.* 2015; Hill *et al.* 2018)) is valuable, recording of EEG during tES is confounded by artifacts (Noury, Hipp, and Siegel 2016; Gebodh *et al.* 2019).

tES electrodes: Dry electrode

Dry electrodes are defined as electrodes that exclude: 1) any saline or other conductive hydrogel-based paste or gel that is prone to leaking; 2) an adhesive at the electrode–skin interface, or 3) any electrode preparation steps. The multilayer hydrogel composite (MHC) electrode design fulfills these criteria (Khadka *et al.* 2018a). A dual layer structure of the MHC dry electrode was adopted by independently optimizing mechanical, electrical, and chemical properties of each layer to get some novel characteristics. First, in order to attain a dry surface, a nonadhesive bio-compatible polymer hydrogel containing polyvinyl alcohol was used as a bottom surface layer (thickness 1 mm) and an adhesive polymer hydrogel was used in an inner layer (thickness 0.6 mm) interfacing a conductive rubber electrode (Fig. 8). The inner layer was optimized to have a low impedance to redistribute the current within the electrode, whereas the bottom layer was optimized to have a high impedance to avoid current clustering at the skin defect sites. Further, pH changes at the nonionic/ionic conduction interface within the electrode were optimized by

using the inner layer as a diffusion barrier and its interface with the rubber electrode was designed to avoid skin surface exposure.

Preliminary analysis of the performance of this MHC electrode using experimental measures on a skin phantom and FEM predictions has shown a comparable voltage and current density distribution under the MHC dry electrode when compared to a conventional sponge electrode. However, the FEM model of the former predicted more homogenous current density distribution at the electrode–skin interface. tDCS using MHC dry electrodes and conventional sponge electrodes was equally tolerated with comparable visual analog scale (VAS) ratings and adverse event reporting. Therefore, MHC electrodes may be a potential alternative of saline soaked sponge electrodes in wearable devices with comparable performance (Khadka *et al.* 2018a).

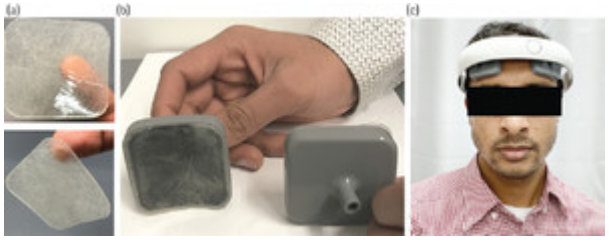

Figure 8 Multilayer hydrogel composite (MHC) dry electrode for tDCS. (A) Images of MHC dry electrode. (B) Illustration of the dry electrode placement under a specialized conductive rubber electrode with the adhesive inner layer facing the rubber and the non-adhesive bottom layer on the opposite side (skin side). The rubber holder is encapsulated in a flexible insulated holder. (C) Images of two MHC dry electrodes secured on the forehead with specialized headgear incorporating a built-in, wearable stimulator.

Erythema may be important for blinding, but it is not directly injurious

Skin redness (erythema) during or after tES is one of the most evident side effects in tES trials (Matsumoto and Ugawa 2017). Like other common adverse effects of limited intensity tES, erythema reflects effects at the skin, and is localized under the electrodes. The causes of tES erythema may include, but are not limited to, exposure to saline, iontophoresis (especially for tDCS), pressure by headgear, and peripheral nerve activation. Redness resolves spontaneously after stimulation and is not injurious. Electrode design and thickness, gender, skin type, nature of stimulation, and intensity of stimulation may mediate erythema intensity and duration (Dundas, Thickbroom, and Mastaglia 2007; Guleyupoglu *et al*. 2013; Guarienti *et al*. 2015).

Recent studies have been conducted to characterize and control tDCS-induced erythema. Brunoni and colleagues previously reported that skin pretreatment with ketoprofen reduces tDCS-induced erythema (Guarienti *et al.* 2015), although such approach inconveniently increases the preparation time. Erythema induced during tDCS varies from mild to moderate. Rater based evaluation of erythema can be overestimated which is solely based on visual inspection of the skin. Hence, a novel approach is to use the collected images for estimating a probability heatmap on the skin area, which presumably represents the erythema distribution under the electrode. This model also corroborates the investigators' observation of skin redness after sham stimulation which might have occurred for reasons such as: 1) the brief period of active stimulation at the session onset; 2) pressure of the pad, depending on how it is fixed; and 3) irritation of the skin due to the saline solution.

Rater-based and software-based data has demonstrated that erythema is very mild after sham stimulation and higher after active stimulation (Fig. 9). Redness did not concentrate around the pad edges, but it was rather diffuse under the electrode (Ezquerro *et al.* 2017). Assuming that the electric current causes redness, it seems that current density is fairly homogeneous below the pad, and redness would be caused by an increase in blood perfusion in the tissue. This contrasts with a previous modeling study that showed that a thin sponge would have the current concentrated in the center of the sponge and a thick sponge—on the edges (Wagner *et al.* 2007). However, that model did not fully capture the inhomogeneity and anisotropy within the skin; for instance, skin or scalp were considered a combined mass of muscle, skin, fat, and connective tissues.

The implications of erythema results in informing tES trial design should be taken with caution. First, the results can be specific to the headgear (e.g., presuming sham erythema reflects pressure), electrode technologies, electrolyte (gel, saline, or cream) used, subject demographics, and waveforms tested. In fact, a prior study has shown dependence on electrode design and skin type. Trial-specific considerations would determine the need and value to mitigate erythema related sham concerns. At a minimum, researchers should be rigorous in controlling and reporting the relevant headgear and electrode, as well as other factors that could induce erythema. Simple methods to conceal exposed skin areas can be implemented. Though not required, erythema intensity can be reduced by treating skin with 2 percent ketoprofen before stimulation (Guarienti *et al.* 2015).

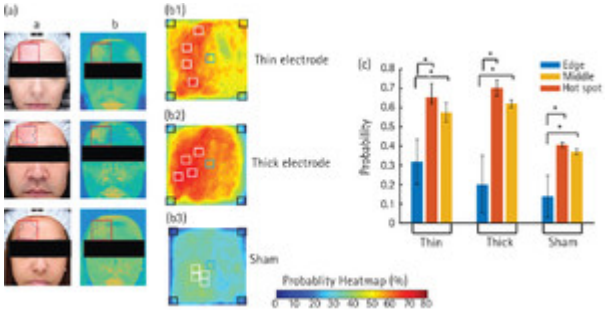

Figure 9 Regional analysis of erythema probability for tDCS with different electrode thicknesses as well as sham. (Aa) Illustration of high definition images of subject photographed after stimulation and demarcation of ROI and traced erythema distribution. (Ab) Representation of filtered images to isolate erythema from regular skin color tone. (B1, B2, B3) Overall erythema probability heatmap and multiple ROIs (edges: black squares, hotspot: white squares, and center: cyan square) defined to contrast the difference in erythema probability across regions. The size of each ROI was 1 percent of the image size. (C) Average erythema intensity for different ROIs (color coded). Erythema at the non-edge regions was higher than at the edges.

Source: Adapted from Fernando Ezquerro, Adriano H. Moffa, Marom Bikson, Niranjan Khadka, Luana V. M. Aparicio, Bernardo de Sampaio-Junior, Felipe Fregni, Isabela M. Bensenor, Paulo A. Lotufo, Alexandre Costa Pereira, and Andre R. Brunoni, The influence of skin redness on blinding in transcranial direct current stimulation studies: A crossover trial. *Neuromodulation: Technology at the Neural Interface*, **20**(3):248–255, https://doi.org/10.1111/ner.12527 © 2016 International Neuromodulation Society.

Electrode resistance

Monitoring of electrode resistance before and during tES is considered important for reproducibility and tolerability (DaSilva *et al.* 2011; Khadka *et al.* 2015), specifically around issues related to electrode setup. An unusually high electrode resistance can indicate undesired electrochemical changes and/or poor skin contact conditions. tES devices therefore include a resistance measurement circuit. However, monitoring of electrode impedance in no way reduces the need and importance of proper electrode selection and setup. Poor electrodes conditions may be associated with a low resistance and, conversely, in some cases (e.g., subjects with high-resistance scalp) good contact may be associated with a moderately high resistance. Skin irritation and discomfort may be associated with high resistance, but not necessarily. Thus, monitoring of resistance is an adjunct tool to

detect nonideal conditions at the electrode–skin interface, and is not a substitute for quality electrode design and strict protocol adherence (Khadka *et al.* 2015; Woods *et al.* 2016).

The resistance measured by the device will be the sum of both electrodes including the underlying electrode–skin resistance, and the body resistance. Body resistance is typically a few kΩ but will vary depending on electrode position on the body and the conditions of the skin (e.g., calloused skin). Electrode–skin resistance will vary depending on the electrode design and waveform applied (Hahn *et al.* 2013). For any given tES device, there will therefore be a specific total resistance range that is considered typical and a resistance above this range may suggest not ideal electrode setup, in which case the operator may adjust the electrode setup to reduce the electrode–skin resistance. Some devices will deactivate it the resistance is atypically high or low.

Current control and voltage limits

Electrodes play a central role in why current control (as opposed to voltage control) is broadly preferred across electrical stimulation applications (Merrill, Bikson, and Jefferys 2005), including tES. Voltage limits, protocols to address voltage compliance, and settings then reflect device specifications. When stimulation is applied to a body from a tES device, the current must pass through electrodes before reaching the body, therefore the electrodes are always in series between the device output and the body. For the simplest case of two electrodes, the total impedance is the sum of the impedance of the two electrodes and the impedance of the body. The impedance of each electrode is unknown, variable over time, changing with the applied current (Khadka *et al.* 2015), and often significant compared to body impedance (Merrill, Bikson, and Jefferys 2005).

First, we consider why voltage control is not preferred. If one used voltage-controlled stimulation, the total voltage provided by the device will be distributed across the two electrodes and the body. But, since the electrode impedances are unknown and changing, the voltage across the body is unknown and changing, and the total current (which reflects the voltage divide by impedance) is also unspecified and changing. Though we are not aware of modern devices that use voltage control in tES, in other brain stimulation applications there may be situations where voltage control is practical, such as stimulation of the vagus nerve through electrode on the neck (GammaCore, Electrocore, NJ, USA), or traditional invasive stimulation technologies such as spinal cord stimulation or deep brain stimulation (DBS) (Medtronic, Fridley, MN, USA).

In contrast, in current controlled stimulation the electrode current is fixed or tracks a specified waveform. The current is passed through the two electrodes and the body, all in series, so the current across the body is controlled. The voltage output of the device is therefore adjusted to keep the current at the target level. The device output voltage divided by the current is the impedance of the system. “Dynamic” impedance refers to the impedance during stimulation as opposed to the “static” impedance measured prior to stimulation (see discussion on resistance in following section). Current control therefore accommodates the unknown, variable, and significant impedance presented by electrodes.

Arguably, with current control one does not know the voltage generated across the body, but this can be predicted knowing the body's resistive properties (see the following discussion of modeling and Thielscher *et al.*, this volume). Moreover, the voltage across the body will not depend on the electrode impedances during current control, but rather will be set by the applied controlled current times the body impedance.

The analogy for why current control provides more specificity of the electricity delivered to the body can be extended to accidental electrical exposure. An individual contacting a high voltage line but wearing insulating rubber gloves would be protected, since the gloves provide a high resistance path in series with the body. Hence, the expression "it's the current, not the voltage, that kills you." While the stimulation intensities used in neuromodulation are much lower than hazardous accidental exposure, and electrodes are designed to be conductive, the analogy is valid in the sense that the electrodes dampen the voltage at the body under voltage-controlled stimulation.

Since under current control, the voltage will increase with the total path resistance, under situations of unusually high resistance, the voltage may increase to the limit of the device, also called device voltage compliance. For limited intensity tES devices, this voltage compliance is typically on the order of tens of volts (e.g., 40 V). The voltage compliance is conventionally set to accommodate passing the maximum target current under expected maximum resistance (e.g., with a target of 2 mA and maximum resistance of 20 kΩ, 40 V is sufficient). In practice, the impedance may increase outside the expected or desired ranges, for example as a result of poor electrode setup. In such cases, the device output may reach the voltage compliance, and the device will not be able to provide the desired current. Depending on the design, devices may respond to voltage compliance in different ways. Some devices may simply abort stimulation, while other devices may continue to stimulate with reduced current. Because current passage itself reduces current (nonlinear and time-variant impedance), maximum impedances are often encountered at the start of stimulation. Therefore, voltage compliance is often increased to accommodate this higher initial impedance. However, given that the impedance would eventually drop, one proposal for limited voltage stimulation was to provide output with moderate voltages, expecting voltage compliance to be reached at the start of stimulation, but for gradual impedance reduction to then reduce the required voltage, allowing target current to be reached (Hahn *et al.* 2013) (Fig. 10). There are various reasons to minimize the output voltage including simplifying circuitry or power requirements, reducing stimulation energy, or providing redundant tolerability measures in susceptible populations or use cases (Gillick *et al.* 2015).

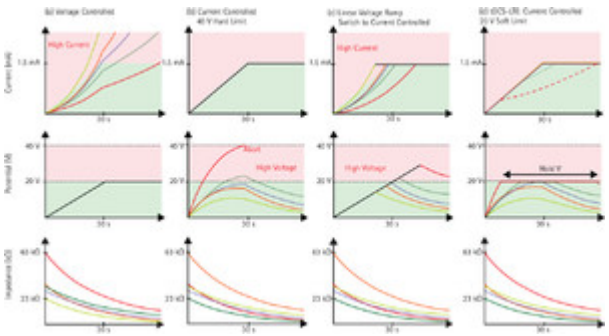

Figure 10 Illustrative example of current, voltage, and impedance trajectories under varied stimulator control schemes. In all four examples, impedance changes for various theoretical subjects (colors) are considered. (A) Voltage controls provide a consistent ramp and steady state voltage level (middle row) but because impedance varied across subjects and time (bottom row) the resulting current is not controlled (top row). (B) Current control with a hard voltage limit regulates current (top row) by adjusting the voltage (middle row) to compensate for changing resistance (bottom row). But, in this regime, if voltage increases to a compliance limit (e.g., 40 V) the stimulation aborts. (C) In a third regime stimulation switched between voltage control and current control. (D) In a fourth regime, LTE, current control is nominally used but when voltage compliance is reached (e.g., 20 V) the stimulation switched to voltage control at this limit. As impedance decreases over time, current control is reengaged.

Source: Adapted from Christoph Hahn, Justin Rice, Shiraz Macuff, Preet Minhas, Asif Rahman, and Marom Bikson, Methods for extra-low voltage transcranial direct current stimulation: Current and time dependent impedance decreases. *Clinical Neurophysiology*, **124**(3):551–556, https://doi.org/10.1016/j.clinph.2012.07.028

Technical comments on resistance in tES including static/dynamic impedance and implications in blinding

How each device measures resistance is an important example of device specification. The electrochemical performance of electrodes, which is the key determinant of resistance or impedance, is complex and has been addressed elsewhere (Merrill, Bikson, and Jefferys 2005). Here, we address the electrode impedance as nonlinear, changing with the applied current intensity and waveform, and varying over time. From a practical perspective, electrode impedance matters as it serves as a quality control tool in essentially all

tES devices. For our purposes here, we consider this impedance to reflect conditions both internal to the electrode (e.g., the metal–gel interface) and at the skin–electrode interface.

The simplest way to minimize skin irritation is through limiting the applied current (e.g., peak current or total charge per session), use of well-designed electrodes (e.g., designed for tES), and following protocols for electrode and skin preparation. Nonetheless, nonideal conditions can arise. Subject reporting of sensation, general observation of electrode and skin conditions, and the monitoring of "electrode resistance" during stimulation (Wagner *et al.* 2007) are conventional methods to monitor electrode conditions. Of these, electrode resistance is the only quantity that is routinely objectively measured. Electrode resistance is thus universally relied on in tES. However, the measured "electrode resistance" is in fact the voltage at the current stimulator output (as the voltage is adjusted to maintain constant current) divided by the applied current. This voltage reflects many nonlinear processes at both electrodes and the tissue. While valuable in tES monitoring, since large excursions in voltage are indicative of nonideal electrode conditions, this is not a primary measure of "skin conditions" nor a measure of single electrode resistance, or even strictly resistance, since electrode over-potentials contribute as well. Sophisticated use of tES can benefit from recognizing the nontriviality of this "electrode resistance" measurement.

Before and after tES, measurement of the "static" resistance requires application of a low-intensity test current. Thus, even prior to stimulation, the resistance reported by a device will speak about the properties of the test current used. Minor variations in the waveform of the test current (e.g., pulses vs dc test waveform, 10 versus 20 μA test current) can significantly change the calculated resistance (Hahn *et al.* 2013). Therefore, the pre/post resistance reported by different tES devices, even under exactly identical electrode and skin contact conditions may vary. Since resistance during stimulation is measured under relatively high current (e.g., 1 mA), the pre/post resistance also does not simply predict resistance during stimulation, though a general correlation is expected (e.g., very high static resistance is associated with high "dynamic" resistance during stimulation). None of this diminishes the value of testing resistance in tES, raising caution about interpreting resistance values in strictly absolute terms.

A relevant effect of tES is that the passage of current itself across the skin may lower the skin dynamic resistance. This means that the effective resistance measured during tES is less than before tES. The source of this resistance drop is likely a decrease in skin impedance (Hahn *et al.* 2013). This feature can be taken advantage of in a situation where it is desired to limit the voltage (energy) generated by a tES device, as illustrated in Fig. 10 (Hahn *et al.* 2013). It also has important consequences for blinding. If the active tES arm produces a distinct current-dependent change in resistance that is absent in the sham arm, then devices that report resistance to the operator during stimulation are not strictly blinded. However, one does not want to remove resistance reporting because of its value as a warning of nonoptimal conditions. One solution is to replace resistance measured during stimulation with more categorical indicators of resistance (e.g., "Good," "Moder-

ate," or "Poor"), that can further be calibrated to be even across active and sham conditions (Brunoni *et al.* 2015; Alonzo *et al.* 2016).

Current flow modeling informs device and electrode design and setup

Computational modeling for tES is considered in detail in Thielscher *et al.*, Chapter 6, this volume. Here, we link modeling to device performance. Electrodes of different size positioned on the scalp along with the current applied to each electrode define tES dose (Peterchev *et al.* 2012). But, it is tES dose in combination with head anatomy that determines the resulting current flow (intensity and pattern) in the brain (Bikson *et al.* 2015; Opitz *et al.* 2016), and therefore the resulting neurophysiological and behavioral changes (Ho *et al.* 2016). The current flow pattern in the head is complex, is not simply "under" the electrodes, and varies across individuals. The task of current flow models is to relate dose (as controlled by the device) and the resulting brain current flow. While dose is what is specified (device configuration), it is the brain current flow (and associated electric field) that theoretically underpins interpretation of outcomes.

For tES, models can reproduce any anatomical electrode montage and positioning systems (e.g., EEG 10–10, neuronavigated) that devices can practically achieve, though functional positioning is complex (e.g., electrode over transcranial magnetic stimulation (TMS) hotspot), unless that information is provided relative to an anatomical reference frame. The degree to which electrode structure is physically represented in tES model varies, with current practices typically representing the electrolyte (e.g., gel sponge), ensuring the electrolyte skin coverage is represented correctly (Datta *et al.* 2009b). Representing the exact details of the metal and conductive rubber components and any insulating support materials is generally not considered relevant in tES models focused on brain current flow. Simulation boundary conditions (typically constant voltage) are applied to the metal, conductive rubber, or surface comprising their interface to the electrolyte. This is a good approximation since the metal or conductive rubber components of the electrodes are much more electrically conductive than the electrolyte or skin. Only those models that are especially concerned with the electrode design and/or the details of the skin current flow patterns represent electrodes with increased detail (Kronberg and Bikson 2012). One modeling report suggests that electrode design may influence significantly current flow patterns in the brain (Opitz *et al.* 2015) but this depends on underlying modeling assumptions, notably ignoring skin response to the applied current. Electrochemistry is not modeled in tES stimulations. Heating is modeled only in papers explicitly concerned with heating (see the following section).

Prospectively, models support optimization of the electrode montage to target specific brain regions (Dmochowski *et al.* 2011; Sadleir *et al.* 2012; Wang *et al.* 2018), which can be done at the population average (a "best" dose across a group) or individual level (a "best" dose for each person). Moreover, electric field models could inform individualization of the stimulation current amplitude. For example, individual models may be able to

predict the TES motor threshold (Edwards *et al.* 2013; Lee *et al.* 2015), ECT seizure threshold (Lee *et al.* 2017), and tDCS modulatory effects (Laakso *et al.* 2019). Retrospectively, models of conventional tES and high-definition tES support testing hypothesis linking brain regions to neurophysiologic or behavioral changes (Bikson *et al.* 2017). This is typically done with a single dose or a limited number of fixed doses applied across a group and can also include individual analysis by considering individual anatomy (Edwards *et al.* 2013; Mikkonen *et al.* 2018; Laakso *et al.* 2019). This can incorporate registering results from current flow models with imaging data (Halko *et al.* 2011).

Changing dose alters the underling brain current flow. Indeed, the canonical studies establishing the neuromodulation actions of tDCS did so by showing effects specific to dose (electrode montage) (Nitsche and Paulus 2000). Systematic studies have characterized brain-state specific (Brunoni *et al.* 2012; Huang *et al.* 2017b; Pan, Zhu, and Li 2019), individual (Datta *et al.* 2012; Wiethoff, Hamada, and Rothwell 2014; Li, Uehara, and Hanakawa 2015, 2015; Labruna *et al.* 2016), and nonmonotonic (e.g., “more is not more” (Batsikadze *et al.* 2013; Giordano *et al.* 2017; Esmaeilpour *et al.* 2018)) dose response. This complexity of tES dose–response is in line with other forms of brain stimulation, while the sensitivity to brain state is consistent with hypothesized mechanisms of action (Bikson *et al.* 2013). In the majority of tES applications, the dose is fixed across individuals. This is in contrast to other common forms of clinical brain stimulation (rTMS, ECT, DBS) where the dose is typically titrated on subject-specific basis. Also, in many approaches that stimulate the head with the intention to activate superficial cranial nerves (e.g., Cefaly, Thync, Caputron, MindGear), the dose is often adjusted by the subject, typically to maximize the current that is still comfortable. Thus, ongoing research on methods to individualize tES dose is warranted (Bikson *et al.* 2012; Gillick *et al.* 2014; Shah-Basak *et al.* 2015, 2015; Dmochowski *et al.* 2017). For example, the dose could be optimized based on each individual’s anatomy so as to maximize for the current reaching a given target (Dmochowski *et al.* 2011). tES intensity can be individualized using current flow models (Caulfield *et al.* 2020b), possibly in combination with suprathreshold (TES/TMS) techniques (Caulfield *et al.* 2020a). Generally, since the physics of current flow is shared among various subthreshold and suprathreshold tES modalities, the threshold current levels for their effects within a subject are expected to correlate. For example, the motor threshold for TES correlates with the seizure threshold in ECT (Peterchev *et al.* 2015).

For tES models to be accurate, they must correctly represent the shape and resistivity of head tissues (e.g., skin, skull, cerebrospinal fluid, brain). Computational models have been developed (Miranda, Lomarev, and Hallett 2006; Wagner *et al.* 2007; Im *et al.* 2008; Datta *et al.* 2009a; Dmochowski *et al.* 2011; Ruffini *et al.* 2014; Truong *et al.* 2014; Opitz *et al.* 2015) and validated (Datta *et al.* 2013b, 2016; Antal *et al.* 2014, 2014; Opitz *et al.* 2016; Huang *et al.* 2017a) over a decade. New approaches invented using computational models, such as high-definition tDCS, have been directly validated (Datta *et al.* 2013b; Edwards *et al.* 2013; Alam *et al.* 2016; Jog *et al.* 2016; Huang *et al.* 2017a) and applied (Caparelli-Daquer *et al.* 2012; Villamar *et al.* 2013b; Wu *et al.* 2018; Reinhart and Nguyen 2019; Weintraub-Brevda and Chua 2019). It is important not to conflate established mon-

tage-specific effects (e.g., “shaping” the outcomes of stimulation (Nitsche *et al.* 2007)) with demonstration of focality (e.g., current delivery to only one small brain region).

Thus, computational models can be viewed as ancillary software used to inform the design, setup, and programming of tES devices, either based on population optimization or individual optimization. Device specifications limit the dose range that can be explored by a model, while, conversely, models can encourage the creation of new device technology. As an example, a home-based system relying on adhesive electrodes would restrict models to explore electrode locations below the hair line (Tyler *et al.* 2015). Conversely, the potential for focal transcranial stimulation was suggested first by models (Datta *et al.* 2009a), but it was not until practical high-definition electrodes were developed (Minhas *et al.* 2010) that approaches to optimize transcranial stimulation using high-definition arrays could be tested.

tES biophysics and mechanisms

The biophysics of tES is considered in more detail in Wang *et al.*, this volume. Here we link the tES mechanisms of action to device performance. While there are naturally open questions about the mechanisms and efficacy of tES for varied indications, the biophysics of tES related to current delivery to the brain and the resulting polarization of neuronal membranes is well established (Salvador *et al.* 2010; Miranda 2013; Rahman, Lafon, and Bikson 2015). The polarization produced by tES is the initial mechanism of action, and subsequent more complex changes in excitability and plasticity are secondary to this polarization (Jackson *et al.* 2016; Modolo *et al.* 2018).

Current that is passed through tES electrodes takes a path through the head determined by the head anatomy and the resistivity of each tissue type. A fraction of the current never crosses the resistive cranium, instead shunting across the relativity conducive (low resistivity) scalp (Datta *et al.* 2013b). Of the current fraction that crosses the skull, a further portion is shunted by the highly conductivity cerebrospinal fluid. The current component that reaches the brain crosses the grey matter and then the white matter. As current crosses brain tissue, it generates an electric field. Neurons are exposed to and consequently stimulated by the local electric field. Generally, the tES current intensity is not the same across different brain regions, and therefore the electric field strength is distributed nonuniformly as well. For conventional tES using two large pad electrodes, the electric field peak may be in a brain region between the electrodes, in some cases leading to suggested placement of the pads across, rather than over a target such the dorsolateral prefrontal cortex (DLPFC) (Seibt *et al.* 2015).

The peak electric field in the brain during 2 mA tES is 0.5–1 V/m based on intra-cranial recording in subjects and validated by current flow models (Datta *et al.* 2016; Opitz *et al.* 2016; Huang *et al.* 2017a). In contrast, ECT applies 800–900 mA of current producing peak electric field up to approximately 300 V/m (Deng, Lisanby, and Peterchev 2011; Lee *et al.* 2016; Bai *et al.* 2017). This contrast is important. Whereas ECT and most of the invasive brain stimulation techniques such as DBS produce high intensity electric fields in

the brain (> 100 V/m), low-intensity tES approaches produce weak electric fields (< 1 V/m). This is well-known and directly supports an intentionally “sub-threshold” modulation mechanism of low-intensity tES techniques such as tDCS (Jackson *et al.* 2016; Krause *et al.* 2017) and tACS (Jefferys *et al.* 2003; Reato *et al.* 2013b; Fröhlich 2015; Liu *et al.* 2018).

Qualitatively, the direction of current flow across the grey matter can be radial inward (from the pial surface toward the grey–white matter boundary), radial outward, or tangential (along the grey matter) (Datta *et al.* 2008). The current flow will polarize a neuron in a compartment-specific manner (i.e., the soma, dendrites, and axon of a single neuron may be polarized differently (Ranck 1975; Tranchina and Nicholson 1986)). The magnitude and direction of the electric field generated in the grey matter determines the polarization of neuronal compartments (Rahman *et al.* 2013). Radial inward current will depolarize the somas of cortical pyramidal neurons by approximately +0.2 mV per V/m of electric field, while radial outward current will hyperpolarize the cortical pyramidal neuron somas by −0.2 mA per V/m (Radman *et al.* 2009). Radial inward and outward current is expected to increase and decrease, respectively, the firing rate of these neurons because of somatic polarization (Creutzfeldt, Fromm, and Kapp 1962; Radman *et al.* 2007). However, each dendritic compartment will be polarized depending on the neuron morphology (Chan, Hounsgaard, and Nicholson 1988; Bikson *et al.* 2004) and the subsequent effects on neuronal excitability can depend on somatic and dendritic polarization (Bikson *et al.* 2004; Kronberg *et al.* 2017). The electric field will polarize axon terminals (synapses) oriented parallel to the field direction by approximately 1 mV per V/m (Chakraborty *et al.* 2018), which can further influence synaptic function (Bikson *et al.* 2004; Fritsch *et al.* 2010; Kabakov *et al.* 2012; Márquez-Ruiz *et al.* 2012) and therefore the net outcome of stimulation. Developments showing orientation- and polarity-specific effects of stimulation with bipolar high-definition tDCS devices, with high-definition electrodes across gyri, indicates translational relevance of directionality (Rawji *et al.* 2018; Hannah, Iacovou, and Rothwell 2019).

The neurophysiological and hence behavioral consequences of tES depend on how this net polarization (across neurons and their compartments) influences excitability and plasticity (Jackson *et al.* 2016). Because low-intensity tES produces only incremental membrane polarization, the cellular effects of low-intensity tES on brain function will further depend on ongoing activity (Bikson *et al.* 2013; Reato *et al.* 2013b; Krause *et al.* 2017; Rahman *et al.* 2017) and may be amplified over time (tens of minutes) (Bindman, Lippold, and Redfearn 1962; Pelletier and Cicchetti 2014; Reato, Bikson, and Parra 2015). The organization of neurons in active networks with emergent properties like oscillations influences the aggregate effects of tES (Reato *et al.* 2010, 2013b, 2013a; Ali, Sellers, and Fröhlich 2013; Schmidt *et al.* 2014, 2014; Bonaiuto and Bestmann 2015). The ultimate consequences of low-intensity tES on macroscopic measures of neurophysiology (e.g., as measured with TMS) and behavior (e.g., as a result of therapy) are complex (Antal *et al.* 2004; Polanía, Nitsche, and Paulus 2011; Filmer, Dux, and Mattingley 2014; Rawji *et al.* 2018; Vöröslakos *et al.* 2018), but ongoing research (De, Bikson, and Bestmann 2013; Antal and Herrmann 2016; Bikson *et al.* 2017; Fertonani and Miniussi 2017; Reed and Cohen 2018) about such changes should not be conflated with the well-established biophysics of cur-

rent flow and the resulting membrane polarization of low-intensity tES. As with any single aspect of brain function and disease, as well as every intervention, open questions remain, which should not be conflated with a lack of scientific basis for tES. Specifically, there is currently enough basic science supporting tES to inform how devices can be designed and programmed in order to test hypothesis related to brain function and therapy (Helfrich *et al.* 2014; Perceval *et al.* 2017; Elsner, Kugler, and Mehrholz 2018; Nguyen, Deng, and Reinhart 2018; Reinhart and Nguyen 2019).

Tolerability of tES devices

The tolerability of any intervention depends not simply on the device and dose, but on protocol including subject inclusion and exclusion (e.g., age, preexisting condition), operator training and certification, ongoing monitoring, and parallel interventions. For example, the scientific consensus that tDCS is safe and tolerated (Poreisz *et al.* 2007; Aparício *et al.* 2016; Bikson *et al.* 2016; Paneri *et al.* 2016; Woods *et al.* 2016; Antal *et al.* 2017; Nikolin *et al.* 2018) is explicitly limited to those protocols tested and medical-grade equipment. Likewise, human trials of tDCS are almost always considered nonsignificant risk (risk comparable to daily activities). But this risk designation—whether made by the FDA, other national organization, or by a local institutional IRB—must be made on a protocol specific basis, emphasizing that recommendation on safety and tolerability cannot be a blanket one for any device, but must also specify the methods of use. ECT protocols (and therefore the use of ECT devices) are considered significant risk.

We can consider three types of risk. The first is related to the intended device integrity, such as an electrical fault or device misuse (e.g., dropping the device on a subject). The second type of risk includes programming the device or electrode positioning in a manner that delivers an undesired dose. Examples of such risks encompass placing the electrodes at a contraindicated location or extending the stimulation duration beyond the recommended limits. The third type of is risk from the intended dose applied, so when the device is functioning and being operated as intended. For example, pain produced by a high current dose is expected from activation of pain axons in the skin. From the perspective of tES device design, features that minimize risk are those that ensure reliable dose delivery and support consistent electrode setup, when used within the limits of established protocols. Medical grade tES devices and accessories that are designed and manufactured to internationally recognized medical standards—regardless of region specific approval for treatment (Fregni *et al.* 2015; Antal *et al.* 2017; Bikson *et al.* 2018)—provide the highest standard of control in regard to reliability, especially in regard to the first type of risk. The second type of risk can be mitigated by designing a device to limit the range of dose that can be applied, for example limiting the maximum programmable current, providing optimized head-hear, or recommending single-use electrodes. The degree of device flexibility may decrease going from lab research systems to in-clinic systems, and to home-based systems. The third risk is not directly mitigated by device design, since it relates to the intended device operation, but is fully determined by applied dose.

Tingling is a common adverse effect reported in low-intensity tES studies (Poreisz *et al.* 2007; Kessler *et al.* 2012) and is well-tolerated (Khadka *et al.* 2018a) (Fig. 11). For low-intensity techniques like tDCS the severity of adverse events is low across all conditions (Brunoni *et al.* 2012). However, the frequency of tingling is significantly higher under thin versus thick sponge stimulation (88 percent versus 64 percent incidence, respectively) (Minhas *et al.* 2010). As discussed previously, electrode size and salinity of sponge electrodes may influence sensation (Dundas, Thickbroom, and Mastaglia 2007). In principle, electrode design must be optimized to reduce the frequency and intensity of tingling and related sensations in clinical trials, which also enhances blinding effectiveness. For this reason, studies which have focused on the effectiveness of tES (tDCS) blinding technique but provided little attention to the electrode design and preparation techniques (including operator training), are of limited generalized value. There is a dissociation between erythema and tingling, tingling being higher under a thin sponge than thick electrodes (Ezquerro *et al.* 2017). A potential reason may be that the thick sponge produces more uniform current density at the skin surface, resulting in evenly diffused erythema distribution and, hence, lower tingling sensation.

Given general discussions on the reliability of sham protocols in tDCS (Kessler *et al.* 2012; Palm *et al.* 2013; Ezquerro *et al.* 2017; Greinacher *et al.* 2019; Fonteneau *et al.* 2019; Turi *et al.* 2019), a commentary on sensation as it relates to sham reliability is warranted. Foremost, the reliability of sham depends on tolerability of the active tES arm, which is determined by electrode design and application protocols. This warrants special consideration of electrodes and selected electrodes optimized for a given tES application (e.g., electrodes that are single use and preprepared for consistency). It is not surprising that using alternative electrode designs or preparation protocols may increase sensation, compromising blinding just for those methods. Second, the success of a sham arm in any given experiment is predicated on the overall study design (including how blinding success is defined) and not only on perfectly replicating side effects. Indeed, since current evidently produces sensation, under sufficiently persnickety experimental design (including increased participant number), subjects will resolve differences between any doses.

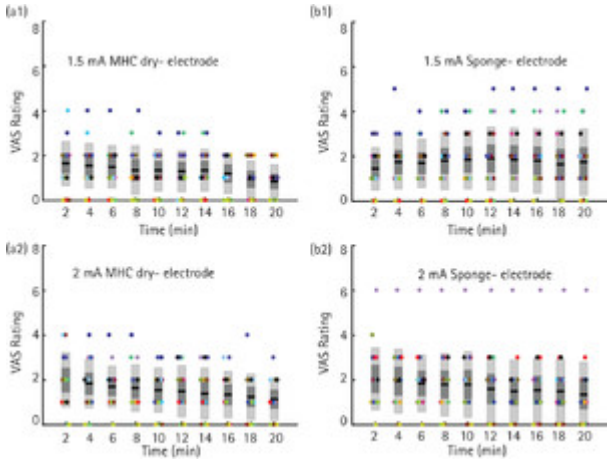

Figure 11 Visual analog scale (VAS) pain score at different stimulation intensities (1.5 mA and 2 mA tDCS) for a conventional sponge and multilayer hydrogel composite (MHC) dry electrode. Participants were color-coded as the cumulative adverse events and relationship to tDCS data, and the VAS pain score (1–10 scale; 1: no pain, 10: unbearable pain) was collected every 2 min during each stimulation sessions. There was no significant different ($P < 0.05$) in the VAS rating across all four stimulation sessions.

Source: Adapted from Niranjan Khadka, Helen Borges, Adantchede L. Zannou, Jongmin Jang, Byunggik Kim, Kiwon Lee, and Marom Bikson, *Brain Stimulation*, 11:5, *Dry tDCS: Tolerability of a Novel Multilayer Hydrogel Composite Non-Adhesive Electrode for Transcranial Direct Current Stimulation*, 1044–1053, doi: 10.1016/j.brs.2018.07.049 Copyright © 2018 Elsevier Inc. with permission from Elsevier.

Heating, no evidence for risk in tES

One of the concerns to be addressed during tES is the potential change in temperature at the skin surface. These changes might theoretically be stimulation waveform specific (e.g., anode or cathode tDCS), and reflecting either joule heating or physiological response to current flow (e.g., due to change in blood perfusion). It has been suggested that small noninjurious changes in skin temperature during tDCS may influence cutaneous sensation (Lagopoulos and Degabriele 2008) and even influence current flow patterns to the brain (DaSilva *et al.* 2011; Gholami-Boroujeny *et al.* 2015). If significant, such changes may also theoretically confound blinding of subjects (e.g., sensation of warmth that is based on real temperature changes) or operators (e.g., in the active case, sponges are warmer). Although higher temperature changes may be injurious and contribute to less tolerable treatment, prior experimental and FEM modeling studies have curtailed a role for significant temperature increases during tDCS. Datta, Elwassif, and Bikson (2009b) predicted no significant temperature rise at the sponge electrode and the scalp interface

deploying 4 × 1 ring high-definition tDCS and conventional tDCS. However, this temperature increase phenomenon was not reported using experimental measures.

A study by Khadka *et al* (Khadka *et al*. 2018b) indicated a moderate and nonhazardous increase in temperature (~ 1°C) at the skin surface during 2 mA tDCS that was independent of polarity, and resulted from stimulation induced blood flow rather than passive heating (Fig. 12). Importantly, this increase was less than the skin cooling produced by application of room temperature electrodes, and any compensatory warming by increased perfusion cannot exceed core temperature. Khadka et al further assessed the alignment of model prediction with the experimental temperature increase during tDCS by sampling ΔT at four different locations (edge-to-edge diagonally) under the sponge pad (at skin surface) in real time (Fig. 13). Experimentally, there was no significant difference in the temperature change ($P > 0.01$) across the locations (i.e., to the resolution of the measurement, the skin under the electrode perimeter did not heat up more than the skin under the center of the electrode). The multi-layer skin model without ultra-structures predicted a nonuniform temperature change across different locations during t = 5 min, 10 min, and 15 min of stimulation. However, near the end time of stimulation (t = 20 min), there was less than 0.01°C temperature change across the different locations, suggesting that the model matches the experimental distribution of temperature near the end of stimulation (t = 20 min) but not near the start time of stimulation (~ t = 5 min). The multi-layer skin model predicted ~ 0.38°C temperature increase due to joule heat (the difference between peak temperature in the active case compared to no stimulation) (t = 20 min), which is less than the experimental measurement of ~ 1.3°C. Since the existing multi-layer skin model lacked ultra-structures such as sweat glands and blood vessels, there was no uniformity in predicted temperature at the skin surface across the early and late time points of stimulation. Therefore, we expect that adding these skin ultra-structures into the existing multi-layer bioheat skin model would increase uniformity of temperature predicted at the skin surface, consistent with the experimental measurement of skin across all time points.

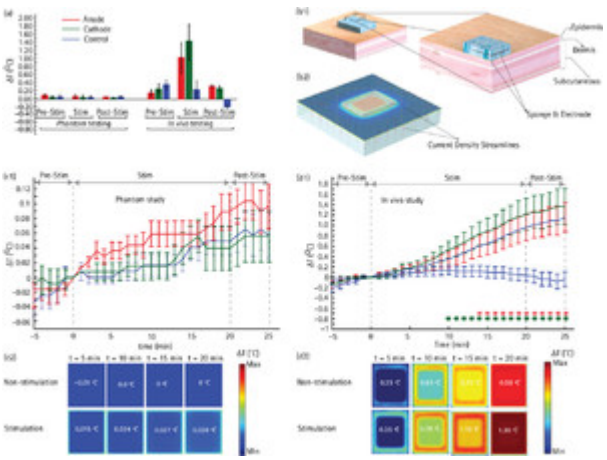

Figure 12 Skin surface temperature increases under tDCS electrodes during pre-stimulation, stimulation, and post-stimulation phases in phantom, in vivo studies, and FEM simulations. (A1) Architecture of a skin model showing three skin layers (epidermis, dermis, and subcutaneous layers) and electrode positioned on the skin surface. (A2) illustrates uniformly seeded current density flow streamlines inside the different skin tissue layers from the top surface of the anode electrode. (B) Average temperature change in subjects (in vivo testing), and phantom (in vitro testing), normalized to temperature at t = 0. In the phantom, ΔT was approximately identical across test samples and mode of stimulation, whereas in the subject testing, maximum ΔT was measured under the active electrode (maximum under cathode) during stimulation. (C1) Analysis of normalized average ΔT in the phantom study (mean ± SEM). No significant difference in ΔT was found in the control, compared to the anode and the cathode. (C2) Predicted ΔT for the non-stimulation (control) and stimulation cases in the phantom FEM model. Predicted findings indicated no significant effect of stimulation on the phantom. (D1) In vivo analysis of temperature difference over time within subjects during pre-stimulation, stimulation, and post-stimulation. Red and green asterisks symbolize statistical significant difference ($P < 0.01$) between anode and control, and cathode and control, respectively. There was a significant difference in ΔT under the anode ($P < 0.01$) and the cathode ($P < 0.01$), compared to the control. Temperature under both anode and cathode gradually increased due to stimulation. (D2) FEM representation of the predicted ΔT in the skin model. A maximum ΔT of 0.38°C was predicted by the computational model during direct current simulation.

Source: Adapted from Niranjan Khadka, Adantchede L. Zannou, Fatima Zunara, Dennis Q. Truong, Jacek Dmochowski, and Marom Bikson, Minimal heating at the skin surface during transcranial direct current stimulation, *Neuromodulation: Technology at the Neural Interface* **214**:334–339, https://doi.org/10.1111/ner.12554 Copyright © 1969, John Wiley and Sons.

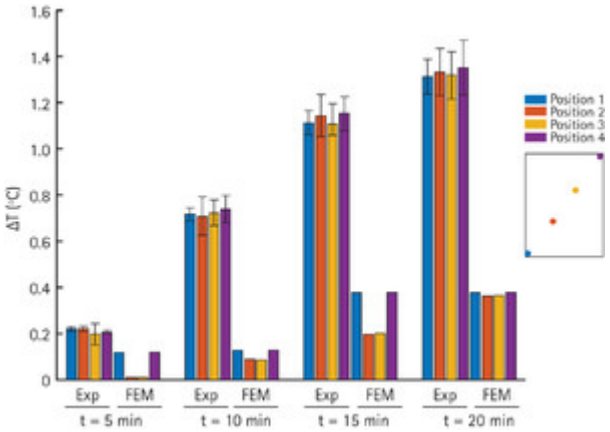

Figure 13 Comparison between experimental temperature increase and predicted temperature increase during 2 mA tDCS at four different locations under the sponge pad for four different time points. The sampling locations are color coded and are sampled from edge-to-edge diagonally. In the case of the experiment, they represent locations for the four thermocouple sensors. The experimental data show temperature measurement for ten subjects (mean ± SEM). The predicted temperature is obtained from a multi-layer skin FEM model without ultrastructures. ΔT is relative to control (no stimulation).

In principle, any electrical stimulation might produce temperature changes, reflecting complex interactions between joule heating due to the applied current across resistive tissue, changes in metabolism (neuronal activation) or perfusion (flare), and heat conduction (Abram, Asiddao, and Reynolds 1980; Elwassif *et al.* 2006). Temperature changes in the body are typically considered insignificant for the efficacy or safety of neuromodulation technologies (Balogun *et al.* 1996; Cramp *et al.* 2000). Skin surface temperature changes of 1°C are noninjurious and within normal variation (e.g., due to exercise, environment) (Scudds, Helewa, and Scudds 1995; Elwassif *et al.* 2006). This certainly appears to be the case for non-invasive electrical stimulation, and situations where it matters to invasive electrical stimulation may reflect stimulation with high rms currents (Zannou *et al.* 2018) or unexpected operation (Elwassif *et al.* 2012). Moreover, as noted, any incremental heating by noninvasive tES is more than compensated by the reduction in surface temperature following application of room-temperature sponges, and since the core body temperature of the blood limits perfusion-based heating, this mechanism is not hazardous. Warmth sensation felt under the tES electrode can thus be attributed to electrical nerve activation rather than heating, and any significant skin irritation (e.g., that occurs only when standard protocols are not followed) is not related to heating but is rather electrochemical in nature (Minhas *et al.* 2010). Any warming of sponges observed by subjects or operators touching the electrode surface would reflect passive heating from the body and it is unlikely that the difference between active and sham can be resolved; hence, this is not an evident confound to blinding.

Practical considerations for placement of electrodes

A central consideration for tES is determining where to place the electrodes on the head (montage). Studies monitoring neurophysiological changes following tES as well as brain current flow FEM prediction and measurements, as previously mentioned, have demonstrated that the relative location of electrodes results in significant differences in where and how much current is delivered in the brain (Minhas *et al.* 2012; Kessler *et al.* 2013; Merlet *et al.* 2013; Woods *et al.* 2015). In some cases, a small variation in the electrode location (distance between the anode electrode and cathode electrode) may significantly alter the overall distribution of the predicted field intensity in the brain (Seibt *et al.* 2015). Thus, proper electrode selection and placement impacts the control and reproducibility of dose (Woods *et al.* 2015). For similar reasons, it is also important that the method of electrode placement and the headgear provide reliable positioning (Seibt *et al.* 2015; Rich and Gillick 2019: 4; Borges *et al.* 2020).

As head size and shape vary from person to person, it is important to use a method for electrode positioning that is robust across individuals. Some techniques for addressing this issue include: 1) International 10–20 (or 10–10 or 10–5) Electrode Placement System (Klem *et al.* 1999; Oostenveld and Praamstra 2001); 2) another gross anatomical coordinate system that may be specific to tES (Seibt *et al.* 2015); 3) neuronavigation systems (e.g., MRI guided) (Feurra *et al.* 2011; Santarnecchi *et al.* 2014); 4) placement based on evoked responses (e.g., location of TES generating MEPs); 5) placement based on functional imaging (e.g., EEG, fMRI). At present, electrode placement based on evoked responses is not common in low-intensity tES since overt responses are not produced, in contrast to TES or TMS. However, TMS can be used to help select tES electrode placement, though this is based on the assumption that placing a tES electrode over a TMS “hot-spot” is optimal. However, these approaches are not exclusive and there is significant interest in refining tES electrode placement technique. For example, the use of EEG to guide (high-definition) tDCS electrode placement has also been investigated (Fernández-Corazza *et al.* 2016; Dmochowski *et al.* 2017).

In general, any positioning technique should specify the center of each electrode along with the electrode shape and orientation. If any special accommodations are made for individual subjects, beyond those already inherent to the positioning technique (e.g., avoiding hairline), dosage adjustments must be noted (Kessler *et al.* 2013). In essence, any positioning method must be clearly documented to allow the protocol to be reproduced. Without rigorous dose documentation, the results of a clinical study (whether positive or negative) are of limited value.

Once desired locations are identified, the electrode assembly must be affixed to the head for delivery of current. Nonconductive headgear used to position the electrodes on the body or scalp (e.g., elastic straps) are critical for appropriate electrode placement (Woods *et al.* 2016). For tES using sponge electrodes, elastic straps (DaSilva *et al.* 2011), or other

specialized headgear (Kasschau *et al.* 2015; Knotkova *et al.* 2019; Borges *et al.* 2020) are used to secure electrodes in place during the entire tES session. Pressure induced erythema can occur even during sham stimulation (Ezquerro *et al.* 2017). Furthermore, if electrode straps are over-tightened, there is an increased probability of saline leakage. Especially with rubber bands (elastic straps) or poorly designed caps, there is a risk with increasing tightening of drift toward the vertex (Woods *et al.* 2015). Specific headgear designs (Kasschau *et al.* 2015; Knotkova *et al.* 2019; Borges *et al.* 2020) prevent drift and can provide more reliable pressure across subjects and operators (Fig. 4). For these reasons, while headgear details are often not reported in detail (make and model, method of positioning), that may impact reproducibility.

With conventional rubber straps, various techniques exist to mitigate the previously mentioned positioning issues. For example, the contour at the base of the skull below the inion and the flat of the forehead provide stable placement of a strap around the head. For participants with long hair, placement of the back of the strap under the hairline also improves stability of the strap preparation, whereas placement over the hair leads to a high probability of upward drift of the strap and the electrodes placed on the head. In totality, the advancement in electrode assembly, particularly electrode straps, can enhance the reproducibility of tES, which can be combined with specialized electrodes that further enhance reliability, as shown in Fig. 4 (Kasschau *et al.* 2015; Knotkova *et al.* 2019; Borges *et al.* 2020).

Historical development of tDCS devices, from re-discovery to home use

We conclude this chapter with a specific description of the historical development of tDCS devices (Fig. 14) and electrodes previously mentioned. This history of electrical stimulation dates to the discovery of electrical phenomena, and static voltage sources are among the earliest examples of electrical stimulation technologies (Paulus and Opitz 2013), though with unclear relation to modern tDCS dose. There has been a continuous history of tES technology development and testing, much of it on non-dc waveforms such as pulsed stimulation (Guleyupoglu *et al.* 2013; Steinberg 2013; Wexler 2017a). Human trials investigating tDCS for neuropsychiatric disorders continued through the middle of the twentieth century, typically with current intensities lower and durations longer than modern tDCS (Esmaeilpour *et al.* 2017). The importance of canonical trials circa 2000 (showing tDCS is a polarity-specific modulator of brain excitability) is evidenced by these trials establishing modern tDCS dose: 1 mA applied over tens of minutes with relatively large electrodes (Nitsche and Paulus 2000, 2001). Subsequent pilot trials instituted a 2 mA intensity for therapeutic interventions (Fregni *et al.* 2005, 2006b, 2006c), which has been maintained for almost all subsequent clinical evaluations (Fregni *et al.* 2006a; Nitsche *et al.* 2008; Bikson *et al.* 2016; Antal *et al.* 2017; Brunoni *et al.* 2017; Lefaucheur *et al.* 2017). These developments established contemporary tDCS dose, and hence the specification of modern tDCS devices. Iontophoresis devices were adopted for some tDCS

trails as an off-label medical device, though they may not provide a steady output (Chhatbar, Sawers, and Feng 2016; Salimpour *et al.* 2016).

Ongoing refinements in dose (e.g., the use of 1.5 mA in cognitive neuroscience (Turkeltaub *et al.* 2012)), electrodes (e.g., high-definition tDCS (Datta *et al.* 2009a)), integration with imaging (e.g., fMRI (Antal *et al.* 2011)), and home-use (e.g., remotely supervised (Charvet *et al.* 2017)) are reflected in specific tDCS device features. Device usability features such as enhanced programming (microcontroller), control systems (e.g., response to impedance changes), rechargeable batteries, disposable electrodes, enhanced headgear materials, wireless connectivity, or integration of monitoring technology (Leite *et al.* 2017), reflect general progress in available technologies but do not alter the delivered tDCS dose.

A theoretical advantage of tDCS is deployability including use in a wide range of clinical environments and at home (Palm *et al.* 2017; Bikson *et al.* 2020; Charvet *et al.* 2020). However, devices designed for use by certified operators at research or clinical centers may not be suitable across deployed conditions. To address this concern, standards for remote-supervised tDCS have been developed (Charvet *et al.* 2015) and validated (Charvet *et al.* 2015; Shaw *et al.* 2017). The principles of remote-supervised tDCS are to operate under continuous medical or research supervision, control compliance, ensure proper dose delivery, and mitigate risk. Features of suitable devices include mechanisms to limit dose (e.g., one 2 mA 20-minute session per day) as well as simple and robust methods to prepare and apply the electrodes (e.g., single use pre-saturated snap electrodes and single position headgear (Fig. 4). While the ethics and merits of self-directed tDCS (outside of medical or research supervision) is debated (Bikson, Paneri, and Giordano 2016; Wexler 2017b; Wagner *et al.* 2018), specifications for tDCS devices that minimize risk have been developed (Bikson *et al.* 2018).

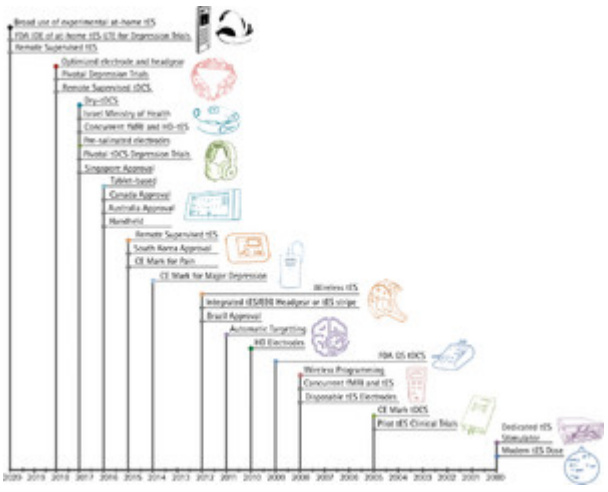

Figure 14 Timeline of modern tDCS innovations: Technology and regulatory milestones.

References

Abram S. E., Asiddao C. B., and Reynolds A. C. (1980) Increased skin temperature during transcutaneous electrical stimulation. *Anesth Analg* **59**:22–25.

Alam M., Truong, D. Q., Khadka N. *et al.* (2016) Spatial and polarity precision of concentric high-definition transcranial direct current stimulation (HD-tDCS). *Phys Med Biol* **61**: 4506.

Ali M. M., Sellers K. K., and Fröhlich F. (2013) Transcranial alternating current stimulation modulates large-scale cortical network activity by network resonance. *J Neurosci* **33**: 11262–11275.

Alonzo A., Aaronson S., Bikson M. *et al.* (2016) Study design and methodology for a multicentre, randomised controlled trial of transcranial direct current stimulation as a treatment for unipolar and bipolar depression. *Contemp Clin Trials* **51**:65–71.

Ambrus G. G., Antal A., and Paulus W. (2011) Comparing cutaneous perception induced by electrical stimulation using rectangular and round shaped electrodes. *Clin Neurophysiol* **122**:803–807.

Antal A., Alekseichuk I., Bikson M. *et al.* (2017) Low intensity transcranial electric stimulation: Safety, ethical, legal regulatory and application guidelines. *Clin Neurophysiol* **128**: 1774–1809.

Antal A., Bikson M., Datta A. *et al.* (2014) Imaging artifacts induced by electrical stimulation during conventional fMRI of the brain. *NeuroImage* 2014;**85 Pt 3**:1040–1047.

Antal A. and Herrmann C. S. (2016) Transcranial alternating current and random noise stimulation: Possible mechanisms. *Neural Plast* doi: 10.1155/2016/3616807.

Antal A., Polania R., Schmidt-Samoa C. *et al.* (2011) Transcranial direct current stimulation over the primary motor cortex during fMRI. *NeuroImage* **55**:590–596.

Antal A., Varga E. T., Kincses T. Z. *et al.* (2004) Oscillatory brain activity and transcranial direct current stimulation in humans. *Neuroreport* **15**:1307–1310.

Aparício L. V. M., Guarienti, F., Razza, L. B. *et al.* (2016) A Systematic review on the acceptability and tolerability of transcranial direct current stimulation treatment in neuropsychiatry trials. *Brain Stimul* **9**:671–681.

Asamoah B., Khatoun A., and Mc Laughlin M. (2019) tACS motor system effects can be caused by transcutaneous stimulation of peripheral nerves. *Nat Commun* **10**:266.

Bai S., Gálvez V., Dokos S. *et al.* (2017) Computational models of Bitemporal, Bifrontal and Right Unilateral ECT predict differential stimulation of brain regions associated with efficacy and cognitive side effects. *Eur Psychiatry* **41**:21–29.

Balogun J. A., Tang S., He Y. *et al.* (1996) Effects of high-voltage galvanic stimulation of ST36 and ST37 acupuncture points on peripheral blood flow and skin temperature. *Disabil Rehabil* **18**:523–528.

Batsikadze G., Moliadze V., Paulus W. *et al.* (2013) Partially non-linear stimulation intensity-dependent effects of direct current stimulation on motor cortex excitability in humans. *J Physiol* **591**:1987–2000.

Bikson M., Brunoni A. R., Charvet L. E. *et al.* (2017) Rigor and reproducibility in research with transcranial electrical stimulation: An NIMH-sponsored workshop. *Brain Stimul* **11**: 3465–3480. doi: 10.1016/j.brs.2017.12.008.

Bikson M., Datta A., Rahman A. *et al.* (2010) Electrode montages for tDCS and weak transcranial electrical stimulation: Role of “return” electrode’s position and size. *Clin Neurophysiol* **121**:1976–1978.

Bikson M., Esmaeilpour Z., Adair D. *et al.* (2019) Transcranial electrical stimulation nomenclature. *Brain Stimul* **12**:1349–1366.

Bikson M., Grossman P., Thomas C. *et al.* (2016) Safety of transcranial direct current stimulation: Evidence based update 2016. *Brain Stimul* **9**:641–661.

Bikson M., Hanlon C. A., Woods A. J. *et al.* (2020) Guidelines for TMS/tES clinical services and research through the COVID-19 pandemic. *Brain Stimul* **13**:1124–1149.

Bikson M., Inoue M., Akiyama H. *et al.* (2004) Effects of uniform extracellular DC electric fields on excitability in rat hippocampal slices in vitro. *J Physiol* **557**:175–190.

Bikson M., Name A., and Rahman A. (2013) Origins of specificity during tDCS: Anatomical, activity-selective, and input-bias mechanisms. *Front Hum Neurosci* **7**:688.

Bikson M., Paneri B., and Giordano J. (2016) The off-label use, utility and potential value of tDCS in the clinical care of particular neuropsychiatric conditions. *J Law Biosci* **3**:642–646.

Bikson M., Paneri B., Mourdoukoutas A. *et al.* (2018) Limited output transcranial electrical stimulation (LOTES-2017): Engineering principles, regulatory statutes, and industry standards for wellness, over-the-counter, or prescription devices with low risk. *Brain Stimul* **11**:134–157.

Bikson M., Rahman A., Datta A. *et al.* (2012) High-resolution modeling assisted design of customized and individualized transcranial direct current stimulation protocols. *Neuromodulation* **15**:306–315.

Bikson M., Truong D. Q., Mourdoukoutas A. P. *et al.* (2015) Modeling sequence and quasi-uniform assumption in computational neurostimulation. *Prog Brain Res* **222**:1–23.

Bindman L. J., Lippold O. C., and Redfearn J. W. (1962) Long-lasting changes in the level of the electrical activity of the cerebral cortex produced bipolarizing currents. *Nature* **196**:584–585.

Bland N. S., Mattingley J. B., and Sale M. V. (2018) No evidence for phase-specific effects of 40 Hz HD-tACS on multiple object tracking. *Front Psychol* **9**:304.

Bonaiuto J. J. and Bestmann S. (2015) Understanding the nonlinear physiological and behavioral effects of tDCS through computational neurostimulation. *Prog Brain Res* **222**:75–103.

Borckardt J. J., Bikson M., Frohman H. *et al.* (2012) A pilot study of the tolerability and effects of high-definition transcranial direct current stimulation (HD-tDCS) on pain perception. *Journal of Pain* **13**:112–120.

Borges H., Dufau A., Paneri B. *et al.* (2020) Updated technique for reliable, easy, and tolerated transcranial electrical stimulation including transcranial direct current stimulation. *JoVE* **155**. doi: 10.3791/59204.

Brunoni A. R., Moffa A. H., Sampaio-Junior B. *et al.* (2017) Trial of electrical direct-current therapy versus escitalopram for depression. *N Engl J Med* **376**:2523–2533.

Brunoni A. R., Nitsche M. A., Bolognini N. *et al.* (2012) Clinical research with transcranial direct current stimulation (tDCS): Challenges and future directions. *Brain Stimul* **5**:175–195.

Brunoni A. R., Sampaio-Junior B., Moffa A. H. *et al.* (2015)The escitalopram versus electric current therapy for treating depression clinical study (ELECT-TDCS): Rationale and study design of a non-inferiority, triple-arm, placebo-controlled clinical trial. *Sao Paulo Med J* **133**:252–263.

Caparelli-Daquer E. M., Zimmermann T. J., Mooshagian E. *et al.* (2012) A pilot study on effects of 4×1 high-definition tDCS on motor cortex excitability. *Conf Proc IEEE Eng Med Biol Soc* **2012**:735–738.

Caulfield K. A., Badran B. W., DeVries W. H. *et al.* (2020a) Transcranial electrical stimulation motor threshold can estimate individualized tDCS dosage from reverse-calculation electric-field modeling. *Brain Stimul* **13**:961–969.

Caulfield K. A., Badran B. W., Li X. *et al.* (2020b) Can transcranial electrical stimulation motor threshold estimate individualized tDCS doses over the prefrontal cortex? Evidence from reverse-calculation electric field modeling. *Brain Stimul* **13**:1150–1152.

Chakraborty D., Truong D. Q., Bikson M. *et al.* (2018) Neuromodulation of Axon Terminals. *Cereb Cortex* **28**:2786–2794.

Chan C. Y., Hounsgaard J., and Nicholson C. (1988) Effects of electric fields on transmembrane potential and excitability of turtle cerebellar Purkinje cells in vitro. *J Physiol* **402**: 751–771

Charvet L. E., Dobbs B., Shaw M. T. *et al.* (2017) Remotely supervised transcranial direct current stimulation for the treatment of fatigue in multiple sclerosis: Results from a randomized, sham-controlled trial. *Mult Scler* **24**:1760–1769. doi: 10.1177/1352458517732842.

Charvet L. E., Kasschau M., Datta A. *et al.* (2015) Remotely supervised transcranial direct current stimulation (tDCS) for clinical trials: Guidelines for technology and protocols. *Front Syst Neurosci* **9**:26.

Charvet L. E., Shaw M. T., Bikson M. *et al.* (2020) Supervised transcranial direct current stimulation (tDCS) at home: A guide for clinical research and practice. *Brain Stimul* **13**: 686–693.

Chhatbar P. Y., Sawers J. R., and Feng W. (2016) The proof is in the pudding: Does tDCS actually deliver DC stimulation? *Brain Stimul* **9**:625–626.

Cramp A. F., Gilsenan C., Lowe A. S., and Walsh D. M. (2000) The effect of high- and low-frequency transcutaneous electrical nerve stimulation upon cutaneous blood flow and skin temperature in healthy subjects. *Clinical Physiology* **20**:150–157.

Creutzfeldt O. D., Fromm G. H., and Kapp H. (1962) Influence of transcortical d-c currents on cortical neuronal activity. *Experimental Neurol* **5**:436–452.

DaSilva A. F., Volz M. S., Bikson M. *et al.* (2011) Electrode positioning and montage in transcranial direct current stimulation. *J Vis Exp* **51**:2744. doi: 10.3791/2744.

Datta A., Bansal V., Diaz J. *et al.* (2009a) Gyri-precise head model of transcranial direct current stimulation: Improved spatial focality using a ring electrode versus conventional rectangular pad. *Brain Stimul* **2**:201–207, 207.e1.

Datta A., Dmochowski J. P., Guleyupoglu B. *et al.* (2013a) Cranial electrotherapy stimulation and transcranial pulsed current stimulation: A computer based high-resolution modeling study. *NeuroImage* **65**:280–287.

Datta A., Elwassif M., Battaglia F. *et al.* (2008). Transcranial current stimulation focality using disc and ring electrode configurations: FEM analysis. *J Neural Eng* **5**:163.

Datta A., Elwassif M., and Bikson M. (2009b) Bio-heat transfer model of transcranial DC stimulation: Comparison of conventional pad versus ring electrode. *Annual International Conference of the IEEE Engineering in Medicine and Biology Society, 2009. EMBC 2009*. 670–673.

Datta A., Krause M. R., Pilly P. K. *et al.* (2016) On comparing in vivo intracranial recordings in non-human primates to predictions of optimized transcranial electrical stimulation. *Conf Proc IEEE Eng Med Biol Soc* **2016**:1774–1777.

Datta A., Truong D., Minhas P. *et al.* (2012) Inter-individual variation during transcranial direct current stimulation and normalization of dose using MRI-derived computational models. *Front Psychiatry* **3**:91.

Datta A., Zhou X., Su Y. *et al.* (2013b) Validation of finite element model of transcranial electrical stimulation using scalp potentials: Implications for clinical dose. *J Neural Eng* **10**:036018.

De A. B., Bikson M., and Bestmann S. (2013) Predicting the behavioral impact of transcranial direct current stimulation: Issues and limitations. *Front Hum Neurosci* **7**:613–613.

De Witte S., Klooster D., Dedoncker J. *et al.* (2018) Left prefrontal neuronavigated electrode localization in tDCS: 10-20 EEG system versus MRI-guided neuronavigation. *Psychiatry Res: Neuroimaging* **274**, doi: 10.1016/j.pscychresns.2018.02.001.

Deng Z-. D, Lisanby S. H., and Peterchev A. V. (2011) Electric field strength and focality in electroconvulsive therapy and magnetic seizure therapy: A finite element simulation study. *J Neural Eng* **8**:016007.

Dmochowski J. P., Datta A., Bikson M. *et al.* (2011) Optimized multi-electrode stimulation increases focality and intensity at target. *J Neural Eng* **8**:046011.

Dmochowski J. P., Koessler L., Norcia A. M. *et al.* (2017) Optimal use of EEG recordings to target active brain areas with transcranial electrical stimulation. *NeuroImage* **157**:69–80.

Dundas J. E., Thickbroom G. W., and Mastaglia, F. L. (2007) Perception of comfort during transcranial DC stimulation: Effect of NaCl solution concentration applied to sponge electrodes. *Clin Neurophysiol* **118**:1166–1170.

Edwards D., Cortes M., Datta A. *et al.* (2013) Physiological and modeling evidence for focal transcranial electrical brain stimulation in humans: A basis for high-definition tDCS. *NeuroImage* **74**:266–275.

Elsner B., Kugler J., and Mehrholz J. (2018) Transcranial direct current stimulation (tDCS) for upper limb rehabilitation after stroke: Future directions. *J Neuroeng Rehabil* **15**:106.

Elwassif M. M., Datt A., Rahman A., *et al.* (2012) Temperature control at DBS electrodes using a heat sink; experimentally validated FEM model of DBS lead architecture. *J Neural Eng* **9**:046009.

Elwassif M. M, Kong Q., Vazquez M. *et al.* (2006) Bio-heat transfer model of deep brain stimulation induced temperature changes. *28th Annual International Conference of the IEEE Engineering in Medicine and Biology Society, 2006. EMBS ’06*, 3580–3583.

Esmaeilpour Z., Marangolo P., Hampstead B. M. *et al.* (2018) Incomplete evidence that increasing current intensity of tDCS boosts outcomes. *Brain Stimul* **11**:310–321.

Esmaeilpour Z., Schestatsky P., Bikson M. *et al.* (2017) Notes on human trials of transcranial direct current stimulation between 1960 and 1998. *Front Hum Neurosci* **11**:71.

Ezquerro F, Moffa A. H., Bikson M. *et al.* (2017) The influence of skin redness on blinding in transcranial direct current stimulation studies: A Crossover Trial. *Neuromodulation* **20**: 248–255.

Fernández-Corazza M., Turovets S., Luu P. *et al.* (2016) Transcranial electrical neuromodulation based on the reciprocity principle. *Front Psychiatry* **7**:87.

Fertonani A, Ferrari C., and Miniussi C. (2015) What do you feel if I apply transcranial electric stimulation? Safety, sensations and secondary induced effects. *Clin Neurophy* **126** :2181–2188 doi: 10.1016/j.clinph.2015.03.015.

Fertonani A. and Miniussi C. (2017) Transcranial electrical stimulation: What we know and do not know about mechanisms. *Neuroscientist* **23**:109–123.

Feurra M., Bianco G., Santarnecchi E. *et al.* (2011) Frequency-dependent tuning of the human motor system induced by transcranial oscillatory potentials. *J Neurosci* **31**:12165–12170.

Feusner J. D., Madsen S., Moody T. D. *et al.* (2012) Effects of cranial electrotherapy stimulation on resting state brain activity. *Brain Behav* **2**:211–220.

Filmer H. L., Dux P. E., and Mattingley J. B. (2014) Applications of transcranial direct current stimulation for understanding brain function. *Trends Neurosci* **37**:742–753.

Fonteneau C., Mondino M., Arns M. *et al.* (2019) Sham tDCS: A hidden source of variability? Reflections for further blinded, controlled trials. *Brain Stimul* **12**:668–673.

Fregni F., Boggio P. S., Lima M. C. *et al.* (2006a) A sham-controlled, phase II trial of transcranial direct current stimulation for the treatment of central pain in traumatic spinal cord injury. *Pain* **122**:197–209.

Fregni F., Boggio P. S., Mansur C. G. *et al.* (2005) Transcranial direct current stimulation of the unaffected hemisphere in stroke patients. *Neuroreport* **16**:1551–1555.

Fregni, F., Boggio P. S., Nitsche M. A. *et al.* (2006b) Treatment of major depression with transcranial direct current stimulation. *Bipolar Disord* **8**:203–204.

Fregni F., Boggio P. S., Santos M. C. *et al.* (2006c) Noninvasive cortical stimulation with transcranial direct current stimulation in Parkinson’s disease. *Mov Disord* **21**:1693–1702.

Fregni F., Nitsche M. A., Loo C. K. *et al.* (2015) Regulatory considerations for the clinical and research use of transcranial direct current stimulation (tDCS): Review and recommendations from an expert panel. *Clin Res Regul Aff* **32**:22–35.

Fritsch B., Reis J., Martinowich K. *et al.* (2010) Direct current stimulation promotes BDNF-dependent synaptic plasticity: Potential implications for motor learning. *Neuron* **66**: 198–204.

Fröhlich F. (2015) Experiments and models of cortical oscillations as a target for noninvasive brain stimulation. *Prog Brain Res* **222**:41–73.

Galletta E. E., Cancelli A., Cottone C. *et al.* (2015) Use of computational modeling to inform tDCS electrode montages for the promotion of language recovery in post-stroke aphasia. *Brain Stimul* **8**:1108–1115.

Garnett E. O., Malyutin S., Datt A. *et al.* (2015) On the use of the terms anodal and cathodal in high-definition transcranial direct current stimulation: A technical note. *Neuromodulation* **18**:705–713.

Gebodh N., Esmaeilpour Z., Adair D. *et al.* (2019) Inherent physiological artifacts in EEG during tDCS. *NeuroImage* **185**:408–424.

George M. S., Taylor J. J., and Short B. (2013) Treating the depressions with superficial brain stimulation methods. *Handb Clin Neurol* **116**:399–413.

Gholami-Boroujeny S., Mekonnen A., Batkin I. *et al.* (2015) Theoretical analysis of the effect of temperature on current delivery to the brain during tDCS. *Brain Stimul* **8**:509–514.

Gillick B. T., Feyma T., Menk J. *et al.* (2015) Safety and feasibility of transcranial direct current stimulation in pediatric hemiparesis: Randomized controlled preliminary study. *Phys Ther* **95**:337–349.

Gillick B. T., Kirton A., Carmel J. B. *et al.* (2014) Pediatric stroke and transcranial direct current stimulation: Methods for rational individualized dose optimization. *Front Hum Neurosci* **8**:739.

Giordano J., Bikson M., Kappenman E. S. *et al.* (2017) Mechanisms and effects of transcranial direct current stimulation. *Dose Response* **15**:1559325816685467.

Greinacher R., Buhôt L., Möller L., and Learmonth G. (2019) The time course of ineffective sham-blinding during low-intensity (1 mA) transcranial direct current stimulation. *Eur J Neurosci* **50**:3380–3388. doi: 10.1111/ejn.14497.

Grossman N., Bono D., Dedic N. *et al.* 2017) Noninvasive deep brain stimulation via temporally interfering electric fields. *Cell* **169**:1029–1041.e16.

Guarienti F., Caumo W., Shiozawa P. *et al.* (2015) Reducing transcranial direct current stimulation-induced erythema with skin pretreatment: Considerations for sham-controlled clinical trials. *Neuromodulation* **18**:261–265.

Guleyupoglu B., Schestatsky P., Edwards D. *et al.* (2013) Classification of methods in transcranial electrical stimulation (tES) and evolving strategy from historical approaches to contemporary innovations. *J Neurosci Methods* **219**:297–311.

Hahn C., Rice J., Macuff S. *et al.* (2013) Methods for extra-low voltage transcranial direct current stimulation: Current and time dependent impedance decreases. *Clin Neurophysiol* **124**:551–556.

Halko M. A., Datta A., Plow E. B., Scaturro J., Bikson M., and Merabet L. B. (2011) Neuroplastic changes following rehabilitative training correlate with regional electrical field induced with tDCS. *Neuroimage* **57**:885–891. doi: 10.1016/j.neuroimage.2011.05.026.

Hannah R., Iacovou A., and Rothwell J. C. (2019) Direction of TDCS current flow in human sensorimotor cortex influences behavioural learning. *Brain Stimul* **12**:684–692.

Heimrath K., Breitling C., Krauel K. *et al.* (2015) Modulation of pre-attentive spectro-temporal feature processing in the human auditory system by HD-tDCS. *Eur J Neurosci* **41**: 1580–1586.

Helfrich R. F., Knepper H., Nolte G. *et al.* (2014) Selective modulation of interhemispheric functional connectivity by HD-tACS shapes perception. *PLoS Biol* **12**:e1002031.

Hill A. T., Rogasch N. C., Fitzgerald P. B. *et al.* (2017) Effects of prefrontal bipolar and high-definition transcranial direct current stimulation on cortical reactivity and working memory in healthy adults. *NeuroImage* **152**:142–157.

Hill A. T., Rogasch N. C., Fitzgerald P. B. *et al.* (2018) Effects of single versus dual-site high-definition transcranial direct current stimulation (HD-tDCS) on cortical reactivity and working memory performance in healthy subjects. *Brain Stimul* **11**:1033–1043.

Ho K-. A., Taylor J. L., Chew T. *et al.* (2016) The effect of transcranial direct current stimulation (tDCS) electrode size and current intensity on motor cortical excitability: Evidence from single and repeated sessions. *Brain Stimul* **9**:1–7.

Huang Y., Liu A. A., Lafon B. *et al.* (2017a) Measurements and models of electric fields in the in vivo human brain during transcranial electric stimulation. *eLife* **6**:e18834.

Huang Y-. Z., Lu M-. K., Antal A. *et al.* (2017b) Plasticity induced by non-invasive transcranial brain stimulation: A position paper. *Clin Neurophysiol* **128**:2318–2329.

Im C. H., Jung H. H., Choi J. D. *et al.* (2008) Determination of optimal electrode positions for transcranial direct current stimulation (tDCS). *Phys Med Biol* **53**:N219–N225.

Jackson, M. P., Rahman A., Lafon B. *et al.* (2016) Animal models of transcranial direct current stimulation: Methods and mechanisms. *Clin Neurophysiol* **127**:3425–3454.

Jefferys J. G. R., Deans J., Bikson M. *et al.* Effects of weak electric fields on the activity of neurons and neuronal networks. *Radiat Prot Dosimetry* 2003;**106**:321–323.

Jog M. V., Smith R. X., Jann K. *et al.* (2016) In-vivo imaging of magnetic fields induced by transcranial direct current stimulation (tDCS) in human brain using MRI. *Sci Rep* **6**: 34385.

Kabakov A. Y., Muller P. A., Pascual-Leone A. *et al.* (2012) Contribution of axonal orientation to pathway-dependent modulation of excitatory transmission by direct current stimulation in isolated rat hippocampus. *J Neurophysiol* **107**:1881–1889.

Kasschau M., Sherman K., Haider L. *et al.* (2015) A protocol for the use of remotely supervised transcranial direct current stimulation (tDCS) in multiple sclerosis (MS). *J Vis Exp* **106**:e53542. doi: 10.3791/53542

Kessler S. K., Minhas P., Woods A. J. *et al.* (2013) Dosage considerations for transcranial direct current stimulation in children: A computational modeling study. *PLOS ONE* **8**:e76112.

Kessler S. K., Turkeltaub P. E., Benson J. G. *et al.* (2012) Differences in the experience of active and sham transcranial direct current stimulation. *Brain Stimul* **5**:155–162.

Khadka N., Borges H., Zannou A. L. *et al.* (2018a) Dry tDCS: Tolerability of a novel multilayer hydrogel composite non-adhesive electrode for transcranial direct current stimulation. *Brain Stimul* **11**:1044–1053.

Khadka N., Rahman A., Sarantos C. *et al.* (2015) Methods for specific electrode resistance measurement during transcranial direct current stimulation. *Brain Stimul* **8**:150–159.

Khadka N., Woods A. J., and Bikson M. (2019) Transcranial direct current stimulation electrodes. In: Knotkova H., Nitsche M. A., Bikson M., *et al.* (eds.) *Practical Guide to Transcranial Direct Current Stimulation: Principles, Procedures and Applications*. Cham: Springer International Publishing, pp. 263–291.

Khadka N., Zannou A. L., Zunara F. *et al.* (2018b) Minimal heating at the skin surface during transcranial direct current stimulation. *Neuromodulation* **21**:334–339.

Klem G. H., Lüders H. O., Jasper H. H. *et al.* (1999) The ten-twenty electrode system of the International Federation. The International Federation of Clinical Neurophysiology. *Electroencephalogr Clin Neurophysiol Suppl* **52**:3–6.

Knotkova H., Riggs A., Berisha D. *et al.* (2019) Automatic M1-SO montage headgear for transcranial direct current stimulation (TDCS) suitable for home and high-throughput in-clinic applications. *Neuromodulation* **22**:904–910.

Krause M. R., Zanos T. P., Csorba B. A. *et al.* (2017) Transcranial direct current stimulation facilitates associative learning and alters functional connectivity in the primate brain. *Curr Biol* **27**:3086–3096.e3.

Kronberg G. and Bikson M. (2012) Electrode assembly design for transcranial direct current stimulation: A FEM modeling study. *Conf Proc IEEE Eng Med Biol Soc* **2012**:891–895.

Kronberg G., Bridi M., Abel T. *et al.* (2017) Direct current stimulation modulates LTP and LTD: Activity dependence and dendritic effects. *Brain Stim* **10**:51–58.

Kuo H. I., Bikson M., Datta A. *et al.* (2013) Comparing cortical plasticity induced by conventional and high-definition 4 ?? 1 ring tDCS: A neurophysiological study. *Brain Stimul* **6**: 644–648.

Laakso I., Mikkonen M., Koyama S. *et al.* (2019) Can electric fields explain inter-individual variability in transcranial direct current stimulation of the motor cortex? *Sci Rep* **9**: 626.

Labruna, L., Jamil, A., Fresnoza, S. *et al.* (2016) Efficacy of anodal transcranial direct current stimulation is related to sensitivity to transcranial magnetic stimulation. *Brain Stimul* **9**:8–15.

Lagopoulos J. and Degabriele R. (2008) Feeling the heat: The electrode–skin interface during DCS. *Acta Neuropsychiatrica* **20**:98–100.

Lee W. H., Lisanby S. H., Laine A. F. *et al.* (2015) Electric field model of transcranial electric stimulation in nonhuman primates: Correspondence to individual motor threshold. *IEEE Trans Biomed Engin* **62**:2095–2105.

Lee W. H., Lisanby S. H., Laine A. F. *et al.* (2016) Comparison of electric field strength and spatial distribution of electroconvulsive therapy and magnetic seizure therapy in a realistic human head model. *Eur Psychiatry* **36**:55–64.

Lee W. H., Lisanby S. H., Laine A. F. *et al.* (2017) Minimum electric field exposure for seizure induction with electroconvulsive therapy and magnetic seizure therapy. *Neuropsychopharmacology* **42**:1192–1200.

Lefaucheur J-. P., Antal A., Ayache S. S. *et al.* (2017) Evidence-based guidelines on the therapeutic use of transcranial direct current stimulation (tDCS). *Clin Neurophysiol* **128**: 56–92.

Leite J., Morales-Quezada L., Carvalho S. *et al.* (2017) Surface EEG-transcranial direct current stimulation (tDCS) closed-loop system. *Int J Neural Syst* **27**:1750026.

Li L. M., Uehara K., and Hanakawa T. (2015) The contribution of interindividual factors to variability of response in transcranial direct current stimulation studies. *Front Cell Neurosci* **9**:181.

Liu A., Vöröslakos M., Kronberg G. *et al.* (2018) Immediate neurophysiological effects of transcranial electrical stimulation. *Nat Commun* **9**:5092.

Márquez-Ruiz J., Leal-Campanario R., Sánchez-Campusano R. *et al.* (2012) Transcranial direct-current stimulation modulates synaptic mechanisms involved in associative learning in behaving rabbits. *Proc Natl Acad Sci USA* **109**:6710–6715.

Matsumoto H. and Ugawa Y. (2017) Adverse events of tDCS and tACS: A review. *Clin Neurophysiol Pract* **2**:19–25.

Meier J., Nolte G., Schneider T. R. *et al.* (2019) Intrinsic 40Hz-phase asymmetries predict tACS effects during conscious auditory perception. *PLoS One* **14**, doi: 10.1371/journal.pone.0213996.

Merlet I., Birot G., Salvador R. *et al.* (2013) From oscillatory transcranial current stimulation to scalp EEG changes: A biophysical and physiological modeling study. *PLoS ONE* **8**:e57330.

Merrill D. R., Bikson M., and Jefferys J. G. R. (2005) Electrical stimulation of excitable tissue: Design of efficacious and safe protocols. *J Neurosci Methods* **141**:171–198.

Mikkonen M., Laakso I., Sumiya M. *et al.* (2018) TMS motor thresholds correlate with TDCS electric field strengths in hand motor area. *Front Neurosci* **12**:426.

Minhas P., Bansal V., Patel J. *et al.* (2010) Electrodes for high-definition transcutaneous DC stimulation for applications in drug-delivery and electrotherapy, including tDCS. *J Neurosci Methods* **190**:188–197.

Minhas P., Bikson M., and Woods A. J. *et al.* (2012) Transcranial direct current stimulation in pediatric brain: A computational modeling study. *Conf Proc IEEE Eng Med Biol Soc* **2012**:859–862.

Minhas P., Datta A., and Bikson M. (2011) Cutaneous perception during tDCS: Role of electrode shape and sponge salinity. *Clin Neurophysiol* **122**:637–638.

Miranda P. C. (2013) Physics of effects of transcranial brain stimulation. *Handb Clin Neurol* **116**:353–366.

Miranda P. C., Lomarev M., and Hallett M. (2006) Modeling the current distribution during transcranial direct current stimulation. *Clin Neurophysiol* **117**:1623–1629.

Modolo J., Denoyer Y., Wendling F. *et al.* (2018) Physiological effects of low-magnitude electric fields on brain activity: Advances from in vitro, in vivo and in silico models. *Curr Opin Biomed Eng* **8**:38–44.

Monte-Silva K., Kuo M-. F., Liebetanz D. *et al.* (2010) Shaping the optimal repetition interval for cathodal transcranial direct current stimulation (TDCS). *J Neurophysiol* **103**:1735–1740. doi: 10.1152/jn.00924.2009.

Nasseri P., Nitsche M. A., and Ekhtiari H. (2015) A framework for categorizing electrode montages in transcranial direct current stimulation. *Front Hum Neurosci* **9**, doi: 10.3389/fnhum.2015.00054.

Nguyen J., Deng Y., and Reinhart R. M. G. (2018) Brain-state determines learning improvements after transcranial alternating-current stimulation to frontal cortex. *Brain Stimul* **11**:723–726.

Nikolin S., Huggins C., Martin D. *et al.* (2018) Safety of repeated sessions of transcranial direct current stimulation: A systematic review. *Brain Stimul* **11**:278–288.

Nitsche M. A., Cohen L. G., Wassermann E. M. *et al.* (2008) Transcranial direct current stimulation: State of the art *Brain Stimul* **1**:206–223.

Nitsche M. A., Doemkes S., Karaköse T. *et al.* (2007) Shaping the effects of transcranial direct current stimulation of the human motor cortex. *J Neurophysiol* **97**:3109–3117.

Nitsche M. A. and Paulus W. (2000) Excitability changes induced in the human motor cortex by weak transcranial direct current stimulation. *J Physiol* **527**:633–639.

Nitsche M. A. and Paulus W. (2001) Sustained excitability elevations induced by transcranial DC motor cortex stimulation in humans. *Neurology* **57**:1899–1901.

Noetscher G. M., Yanamadala J., Makarov S. N. *et al.* (2014) Comparison of cephalic and extracephalic montages for transcranial direct current stimulation—a numerical study. *IEEE Trans Biomed Eng* **61**:2488–2498.

Noury N., Hipp J. F., and Siegel M. (2016) Physiological processes non-linearly affect electrophysiological recordings during transcranial electric stimulation. *Neuroimage* **140**:99–109.

Oostenveld R. and Praamstra P. (2001) The five percent electrode system for high-resolution EEG and ERP measurements. *Clin Neurophysiol* **112**:713–719.

Opitz A., Falchier A., Yan C-. G. *et al.* (2016) Spatiotemporal structure of intracranial electric fields induced by transcranial electric stimulation in humans and nonhuman primates. *Scientific Reports* **6**:srep31236.

Opitz A., Paulus W., Will S. *et al.* (2015) Determinants of the electric field during transcranial direct current stimulation. *Neuroimage* **109**:140–150.

Palm U., Kumpf U., Behler N. *et al.* (2017) Home use, remotely supervised, and remotely controlled transcranial direct current stimulation: A systematic review of the available evidence. *Neuromodulation* **21**:323–333. doi: 10.1111/ner.12686.

Palm U., Reisinger E., Keeser D. *et al.* (2013) Evaluation of sham transcranial direct current stimulation for randomized, placebo-controlled clinical trials. *Brain Stim* **6**:690–695.

Pan J., Zhu C., and Li J. (2019) Uncertainty modulates the effect of transcranial stimulation over the right dorsolateral prefrontal cortex on decision-making under threat. *Front Neurosci* **13**:305.

Paneri B., Adair D., Thomas C. *et al.* (2016) Tolerability of repeated application of transcranial electrical stimulation with limited outputs to healthy subjects. *Brain Stimul* **9**: 740–754.

Parazzini M., Fiocchi S., Cancelli A. *et al.* (2017) A computational model of the electric field distribution due to regional personalized or non-personalized electrodes to select transcranial electric stimulation target. *IEEE Trans Biomed Eng* **64**:184–195.

Paulus W. and Opitz A. (2013) Ohm's law and tDCS over the centuries. *Clin Neurophysiol* **124**:429–430.

Pelletier S. J. and Cicchetti F. (2014) Cellular and molecular mechanisms of action of transcranial direct current stimulation: Evidence from in vitro and in vivo models. *Int J Neuropsychopharmacol* **18**, doi: 10.1093/ijnp/pyu047.

Perceval, G., Martin A. K., Copland, D. A. *et al.* (2017) High-definition tDCS of the temporo-parietal cortex enhances access to newly learned words. *Sci Rep* **7**:17023–17023.

Peterchev A. V., Krystal A. D., Rosa M. A. *et al.* (2015) Individualized low-amplitude seizure therapy: Minimizing current for electroconvulsive therapy and magnetic seizure therapy. *Neuropsychopharmacology* **40**:2076–2084.

Peterchev A. V., Rosa M. A., Deng Z-. D. *et al.* (2010) Electroconvulsive therapy stimulus parameters: Rethinking dosage. *J ECT* **26**:159–174.

Peterchev A. V., Wagner T. A., Miranda P. C. *et al.* (2012) Fundamentals of transcranial electric and magnetic stimulation dose: Definition, selection, and reporting practices. *Brain Stimul* **5**:435–453.

Polanía R., Nitsche M. A., and Paulus W. (2011) Modulating functional connectivity patterns and topological functional organization of the human brain with transcranial direct current stimulation. *Hum Brain Mapp* **32**:1236–1249.

Poreisz C., Boros K., Antal A. *et al.* (2007) Safety aspects of transcranial direct current stimulation concerning healthy subjects and patients. *Brain Res Bull* **72**:208–214.

Radman T., Ramos R. L., Brumberg J. C. *et al.* (2009) Role of cortical cell type and morphology in subthreshold and suprathreshold uniform electric field stimulation in vitro. *Brain Stimul* **2**:215–228, 228 e1–e3.

Radman T., Su, Y., An J. H. *et al.* (2007) Spike timing amplifies the effect of electric fields on neurons: Implications for endogenous field effects. *J Neurosci* **27**:3030–3036.

Rahman A., Lafon B., and Bikson M. (2015) Multilevel computational models for predicting the cellular effects of noninvasive brain stimulation. *Prog Brain Res* **222**:25–40.

Rahman A., Lafon B., Parra L. C. *et al.* (2017) Direct current stimulation boosts synaptic gain and cooperativity in vitro. *J Physiol (Lond)* **595**:3535–3547.

Rahman A., Reato D., Arlotti M. *et al.* (2013) Cellular effects of acute direct current stimulation: Somatic and synaptic terminal effects. *J Physiol (Lond)* **591**:2563–2578.

Ranck J. B. (1975) Which elements are excited in electrical stimulation of mammalian central nervous system: A review. *Brain Res* **98**:417–440.

Rawji V., Ciocca M., Zacharia A. *et al.* (2018) tDCS changes in motor excitability are specific to orientation of current flow. *Brain Stimul* **11**:289–298.

Reato D., Bikson M., and Parra, L. C. (2015) Lasting modulation of in vitro oscillatory activity with weak direct current stimulation. *J Neurophysiol* **113**:1334–1341.

Reato D., Gasca F., Datta A. *et al* (2013a) Transcranial electrical stimulation accelerates human sleep homeostasis. *PLoS Comput Biol* **9**: e1002898–e1002898.

Reato D., Rahman A., Bikson M. *et al.* (2010) Low-intensity electrical stimulation affects network dynamics by modulating population rate and spike timing. *J Neurosci* **30**:15067–15079.

Reato D., Rahman A., Bikson M. *et al.* (2013b) Effects of weak transcranial alternating current stimulation on brain activity-a review of known mechanisms from animal studies. *Front Hum Neurosci* **7**:687.

Reed T. and Cohen R. K. (2018) Transcranial electrical stimulation (tES) mechanisms and its effects on cortical excitability and connectivity. *J Inherit Metab Dis* **41**:1123–1130. doi: 10.1007/s10545-018-0181-4.

Reinhart R. M. G. and Nguyen J. A. (2019) Working memory revived in older adults by synchronizing rhythmic brain circuits. *Nat Neurosci* **22**:820–827.

Rich T. L. and Gillick B. T. (2019) Electrode placement in transcranial direct current stimulation—how reliable is the determination of C3/C4? *Brain Sci* **9**, doi: 10.3390/brainsci9030069.

Rich T. L., Menk J. S., Rudse, K. D. *et al.* (2017) Determining electrode placement for transcranial direct current stimulation: A comparison of EEG- versus TMS-guided methods. *Clin EEG Neurosci* **48**:367–375.

Richardson J., Datta A., Dmochowski J. *et al.* (2015) Feasibility of using high-definition transcranial direct current stimulation (HD-tDCS) to enhance treatment outcomes in persons with aphasia. *Neuro Rehabilitation* **36**:115–126.

Ruffini G., Fox M. D., Ripolles O. *et al.* (2014) Optimization of multifocal transcranial current stimulation for weighted cortical pattern targeting from realistic modeling of electric fields. *NeuroImage* **89**:216–225.

Sadleir R. J., Vannorsdall T. D., Schretlen D. J. *et al.* (2012) Target optimization in transcranial direct current stimulation. *Front Psychiatry* **3**:90–90.

Salimpour Y., Wei Z., Duy P. Q. *et al.* (2016) Does transcranial direct current stimulation actually deliver dc stimulation? *Brain Stim* **9**:623–624.

Salvador R., Mekonnen A., Ruffini G. *et al.* (2010) Modeling the electric field induced in a high-resolution realistic head model during transcranial current stimulation. *Conf Proc IEEE Eng Med Biol Soc* **2010**:2073–2076.

Santarnecchi E., Feurra M., Barnesch, F. *et al.* (2014) Time course of corticospinal excitability and autonomic function interplay during and following monopolar tDCS. *Front Psychiatry* **5**:86.

Schestatsky P., Morales-Quezada L., and Fregni F. (2013) Simultaneous EEG monitoring during transcranial direct current stimulation. *J Vis Exp* **76**:50426.

Schmidt S. L., Iyengar A. K., Foulser A. A. *et al.* (2014) Endogenous cortical oscillations constrain neuromodulation by weak electric fields. *Brain Stimul* **7**:878–889.

Scudds R. J., Helewa A., Scudds R. A. (1995) The effects of transcutaneous electrical nerve stimulation on skin temperature in asymptomatic subjects. *Phys Ther* **75**:621–628.

Seibt O., Brunoni A. R., Huang Y. *et al.* (2015) The pursuit of DLPFC: Non-neuronavigated methods to target the left dorsolateral pre-frontal cortex with symmetric bicephalic transcranial direct current stimulation (tDCS). *Brain Stimul* **8**:590–602.

Shah-Basak P. P., Norise C., Garcia G. *et al.* (2015) Individualized treatment with transcranial direct current stimulation in patients with chronic non-fluent aphasia due to stroke. *Front Hum Neurosci* **9**:201.

Shaw M. T., Kasschau M., Dobbs B. *et al.* (2017) Remotely supervised transcranial direct current stimulation: An update on safety and tolerability. *J Vis Exp* **128**:56211. doi: 10.3791/56211.

Shen B., Yin Y., and Wang J. *et al.* (2016) High-definition tDCS alters impulsivity in a baseline-dependent manner. *NeuroImage* **143**:343–352.

Steinberg H. (2013) Letter to the editor: Transcranial direct current stimulation (tDCS) has a history reaching back to the 19th century. *Psychol Med* **43**:669–671.

Teichmann M., Lesoil C., Godard J. *et al.* (2016) Direct current stimulation over the anterior temporal areas boosts semantic processing in primary progressive aphasia. *Ann Neurol* **80**:693–707.

Thut G., Bergmann T. O., Fröhlich F. *et al.* (2017) Guiding transcranial brain stimulation by EEG/MEG to interact with ongoing brain activity and associated functions: A position paper. *Clin Neurophysiol* **128**:843–857.

Tranchina D. and Nicholson C. (1986) A model for the polarization of neurons by extrinsically applied electric fields. *Biophys J* **50**:1139–1156.

Truong D. Q., Hüber M., Xie X. *et al.* (2014) Clinician accessible tools for GUI computational models of transcranial electrical stimulation: BONSAI and SPHERES. *Brain Stimul* **7**:521–524.

Turi Z., Ambrus G. G., Ho K-. A. *et al.* (2014) When size matters: Large electrodes induce greater stimulation-related cutaneous discomfort than smaller electrodes at equivalent current density. *Brain Stimul* **7**:460–467.

Turi Z., Ambrus G. G., Janacsek K. *et al.* (2013) Both the cutaneous sensation and phosphene perception are modulated in a frequency-specific manner during transcranial alternating current stimulation. *Restorative Neurol Neurosci* **31**:275–285.

Turi Z., Csifcsák G., Boayue N. M. *et al.* (2019) Blinding is compromised for transcranial direct current stimulation at 1 mA for 20 min in young healthy adults. *Eur J Neurosci* **50**: 3261–3268. doi: 10.1111/ejn.14403.

Turkeltaub P. E., Benson J., Hamilton R. H. *et al.* (2012) Left lateralizing transcranial direct current stimulation improves reading efficiency. *Brain Stim* **5**:201–207.

Tyler W. J., Boasso A. M., Mortimore H. M. *et al.* (2015) Transdermal neuromodulation of noradrenergic activity suppresses psychophysiological and biochemical stress responses in humans. *Scientific Reports* **5**:13865.

Villamar M. F., Volz M. S., Bikson M. *et al.* (2013a) Technique and considerations in the use of 4x1 ring high-definition transcranial direct current stimulation (HD-tDCS). *J Vis Exp* **77**:e50309.

Villamar M. F., Wivatvongvana P., Patumanond J. *et al.* (2013b) Focal modulation of the primary motor cortex in fibromyalgia using 4×1-ring high-definition transcranial direct current stimulation (HD-tDCS): Immediate and delayed analgesic effects of cathodal and anodal stimulation. *J Pain* **14**:371–383.

Vöröslakos M., Takeuchi Y., Brinyiczki K. *et al.* (2018) Direct effects of transcranial electric stimulation on brain circuits in rats and humans. *Nat Commun* **9**:483.

Wagner K., Maslen H., Oakley J. *et al.* (2018) Would you be willing to zap your child's brain? Public perspectives on parental responsibilities and the ethics of enhancing children with transcranial direct current stimulation. *AJOB Empir Bioeth* **9**:29–38.

Wagner S., Lucka F., Vorwerk J. *et al.* (2016) Using reciprocity for relating the simulation of transcranial current stimulation to the EEG forward problem. *NeuroImage* **140**:163–173.

Wagner T., Fregni F., Fecteau S. *et al.* (2007) Transcranial direct current stimulation: A computer-based human model study. *NeuroImage* **35**:1113–1124.

Wang Y., Zhou H., Li Y. *et al.* (2018) Impact of electrode number on the performance of high-definition transcranial direct current stimulation (HD-tDCS). *Conf Proc IEEE Eng Med Biol Soc* 2018; 4182–4185.

Weintraub-Brevda R. R. and Chua E. F. (2019) Transcranial direct current stimulation over the right and left VLPFC leads to differential effects on working and episodic memory. *Brain Cogn* **132**:98–107.

Wexler A. (2017a) Recurrent themes in the history of the home use of electrical stimulation: Transcranial direct current stimulation (tDCS) and the medical battery (1870–1920). *Brain Stimul* **10**:187–195.

Wexler A. (2017b) The social context of “do-it-yourself” brain stimulation: Neurohackers, biohackers, and lifehackers. *Front Hum Neurosci* **11**:224.

Wiethoff S., Hamada M., and Rothwell J. C. (2014) Variability in response to transcranial direct current stimulation of the motor cortex. *Brain Stimul* **7**:468–475.

Woods A. J., Antal A., Bikson M. *et al.* (2016) A technical guide to tDCS, and related non-invasive brain stimulation tools. *Clin Neurophysiol* **127**:1031–1048.

Woods A. J., Bryant V., Sacchetti D. *et al.* (2015) Effects of electrode drift in transcranial direct current stimulation. *Brain Stimul* **8**:515–519.

Wu X., Xu F., Chen X. *et al.* (2018) The effect of high-definition transcranial direct current stimulation of the right inferior frontal gyrus on empathy in healthy individuals. *Front Hum Neurosci* **12**:446.

Zannou A. L., Khadka N., Truong D. Q. *et al.* (2018) Temperature increases by kilohertz frequency spinal cord stimulation. *Brain Stimul* **12**:62–72. doi: 10.1016/j.brs.2018.10.007.

Dennis Q. Truong

Biomedical Engineering, The City College of the City University of New York

Niranjan Khadka

Department of Biomedical Engineering, The City College of New York, CUNY

Angel V. Peterchev

Duke University Medical Center, Department of Psychiatry & Behavioral Sciences

Transcranial electrical stimulation devices

Marom Bikson

Biomedical Engineering, The City College of the City University of New York